Microbiological Research 286 (2024) 127816

Contents lists available at ScienceDirect

Microbiological Research

journal homepage: www.elsevier.com/locate/micres

Deciphering the mechanisms involved in reduced sensitivity to azoles and fengycin lipopeptide in *Venturia inaequalis*

Aline Leconte [a,b,c], Justine Jacquin [a], Matthieu Duban [b], Caroline Deweer [a], Pauline Trapet [a], Frédéric Laruelle [d], Amaury Farce [e], Philippe Compère [f], Karin Sahmer [g], Valentin Fiévet [a], Alexis Hoste [c], Ali Siah [a], Anissa Lounès-Hadj Sahraoui [d], Philippe Jacques [c], François Coutte [b], Magali Deleu [c], Jérôme Muchembled [a,*]

[a] *JUNIA, UMRt BioEcoAgro 1158-INRAE, Plant Secondary Metabolites Team, Charles Viollette Institute, Lille F-59000, France*
[b] *University of Lille, UMRt BioEcoAgro 1158-INRAE, Microbial Secondary Metabolites team, Charles Viollette Institute, Lille F-59000, France*
[c] *University of Liège, UMRt BioEcoAgro 1158-INRAE, Microbial Secondary Metabolites team, TERRA Teaching and Research Centre, Gembloux Agro-Bio Tech, Gembloux B-5030, Belgium*
[d] *Unité de Chimie Environnementale et Interactions sur le Vivant (EA 4492), Université Littoral Côte d'Opale, CEDEX CS 80699, Calais 62228, France*
[e] *Université Lille, Inserm, CHU Lille, U1286 - INFINITE - Institut de recherche translationnelle sur l'inflammation, Lille F-59000, France*
[f] *Laboratoire de morphologie fonctionnelle et évolutive, UR FOCUS, and Centre de recherche appliquée et d'enseignement en microscopie (CAREM), Université de Liège, Liège, Belgium*
[g] *Université Lille, IMT Lille Douai, Univ. Artois, JUNIA, ULR 4515 - LGCgE, Laboratoire de Génie Civil et geo-Environnement, Lille F-59000, France*

ARTICLE INFO

Key words:
Venturia inaequalis
Azoles
Lipopeptides
Bacillus sp.
Antifungal activity
Lipids

ABSTRACT

Apple scab, caused by the hemibiotrophic fungus *Venturia inaequalis*, is currently the most common and damaging disease in apple orchards. Two strains of *V. inaequalis* (S755 and Rs552) with different sensitivities to azole fungicides and the bacterial metabolite fengycin were compared to determine the mechanisms responsible for these differences. Antifungal activity tests showed that Rs552 had reduced sensitivity to tebuconazole and tetraconazole, as well as to fengycin alone or in a binary mixture with other lipopeptides (iturin A, pumilacidin, lichenysin). S755 was highly sensitive to fengycin, whose activity was close to that of tebuconazole. Unlike fengycin, lipopeptides from the iturin family (mycosubtilin, iturin A) had similar activity on both strains, while those from the surfactin family (lichenysin, pumilacidin) were not active, except in binary mixtures with fengycin. The activity of lipopeptides varies according to their family and structure. Analyses to determine the difference in sensitivity to azoles (which target the CYP51 enzyme involved in the ergosterol biosynthesis pathway) showed that the reduced sensitivity in Rs552 is linked to (i) a constitutive increased expression of the *Cyp51A* gene caused by insertions in the upstream region and (ii) greater efflux by membrane pumps with the involvement of ABC transporters. Microscopic observations revealed that fengycin, known to interact with plasma membranes, induced morphological and cytological changes in cells from both strains. Sterol and phospholipid analyses showed a higher level of ergosta-7,22-dien-3-ol and a lower level of PI(C16:0/C18:1) in Rs552 compared with S755. These differences could therefore influence the composition of the plasma membrane and explain the differential sensitivity of the strains to fengycin. However, the similar antifungal activities of mycosubtilin and iturin A in the two strains indirectly indicate that sterols are probably not involved in the fengycin resistance mechanism. This leads to the conclusion that different mechanisms are responsible for the difference in susceptibility to azoles or fengycin in the strains studied.

1. Introduction

Apple scab, caused by the phytopathogenic fungus *Venturia inaequalis*, is the disease that causes the most agro-economic losses for apple growers. Scab affects the plant mainly during its growth, in particular the fruit and leaves. Symptoms on the fruit are visible in the form of black spots, making the fruit unmarketable (Bowen et al., 2011). One of the fungicide families most commonly used against apple scab is the

* Corresponding author.
E-mail address: jerome.muchembled@junia.com (J. Muchembled).

https://doi.org/10.1016/j.micres.2024.127816
Received 23 April 2024; Received in revised form 6 June 2024; Accepted 20 June 2024
Available online 27 June 2024

azoles (Cordero-Limon et al., 2020).This family belongs to the group of demethylation inhibitors (DMIs) that target the biosynthesis of fungal sterols. Azoles target the C14-demethylase enzyme (CYP51) encoded by the *Cyp51A* gene, which is essential for the biosynthesis of sterols such as ergosterol (Price et al., 2015; Villani et al., 2016). Ergosterol is a component required for the regulation of cell membrane stability in eukaryotes and is considered a fingerprint of fungi (Ermakova and Zuev, 2017; Stephenson, 2010). Due to the frequent use of DMIs to control apple scab, few cases of fungicide resistance have been observed in orchards. Resistance to fenbuconazole (Xu et al., 2010), to myclobutanil and difenoconazole (Villani et al., 2015) and to tebuconazole (Cordero-Limon et al., 2020) has been reported in *V. inaequalis*. Azole resistance is also well known in other fungi, such as *Penicillium digitatum* (Hamamoto et al., 2000; Sun et al., 2013), *Zymoseptoria tritici* (Cools and Fraaije, 2013) and *Puccinia tritici* (Stammler et al., 2009) for example. As azoles inhibit the C14-demethylase enzyme by binding to it, several studies on the *Cyp51A* gene and its relationship with azole resistance have been carried out in several plant pathogenic fungi. Overall, three mechanisms could explain resistance to azoles (Price et al., 2015): (i) the appearance of point mutations in the *Cyp51A* gene (Yaegashi et al., 2020), (ii) increased expression of the *Cyp51A* gene (Villani et al., 2016) and/or (iii) increased expression of genes coding for ABC efflux pumps (ATP-Binding Cassette) and MFS (Major Facilitator Superfamily) types efflux pumps (Hulvey et al., 2012). Mutations in *Cyp51A* are the most frequently reported mechanism of resistance. Mutations involving amino-acid substitutions can alter the affinity between the fungicide and the targeted enzyme. Increased expression of the *Cyp51A* gene leads to an increase in the quantity of the C14-demethylase enzyme, thereby increasing sterol production. Finally, ABC transporters and MFS pumps give fungal cells the ability to reject undesirable molecules such as azoles. The efflux pump mechanism is responsible for multidrug resistance (MDR) conferring cross-resistance to fungicides from different chemical families (Price et al., 2015). The level of resistance can vary depending on the fungicide family used. For strobilurins that inhibit fungal respiration, resistance (caused by the G143A substitution in the mitochondrial cytochrome b enzyme) is disruptive because fungal genotypes can be fully sensitive (wild type) or fully resistant within fungal populations (Cheval et al., 2017). In contrast, in the case of azoles, resistance is 'progressive' as a gradient of resistance occurs within populations. Such resistance behaviour is often referred to as 'reduced sensitivity' rather than 'resistance', as only a decrease in fungicide sensitivity is observed and no complete resistance occurs in fungal populations in the field (Villani et al., 2015). Despite the agroeconomic importance of apple scab, the molecular basis of azole resistance mechanisms in *V. inaequalis* is poorly studied and the efflux-pump-based mechanism has never been investigated.

In the current context of agroecology and sustainable agriculture, the search for alternatives to fungicides, such as the use of biochemical compounds, is widely encouraged (Falardeau et al., 2013). Lipopeptides produced by *Bacillus spp*, beneficial soil bacteria, are promising biomolecules for controlling apple scab (Leconte et al., 2022) and their use could potentially reduce or replace the use of synthetic chemical fungicides in orchards. Lipopeptides are biodegradable and have been shown to have antifungal activity (Desmyttere et al., 2019; Moyne et al., 2001) and properties that stimulate plant defence (Cawoy et al., 2014; Chowdhury et al., 2015; Rahman et al., 2015). They have been shown to interact with membrane lipids and/or sterols (Aranda et al., 2005; Deleu et al., 2005, 2008; Maget-Dana and Peypoux, 1994). There are more than 1500 different lipopeptide structures divided into three main families: fengycins, iturins and surfactins (Jacques, 2011). Fengycins are composed of ten amino acids, eight of which form the peptide ring, and a β-hydroxy fatty acid chain. Iturins are composed of seven amino acids forming a lactam peptide ring with a β-amino fatty acid chain. Both fengycins and iturins can alter membranes by permeabilising them, forming ionic pores (Aranda et al., 2005, 2023; Zakharova et al., 2019). Finally, surfactins are heptapeptides, forming a lactone ring with a β-hydroxylated fatty acid chain. Highly amphiphilic, surfactins can interact with the membrane by inserting themselves into lipid bilayers but without forming pores (Ongena and Jacques, 2008).

In a previous work, two strains of *V. inaequalis* were examined for their sensitivity to tebuconazole and fengycin (Desmyttere et al., 2019). Interestingly, strain Rs552 showed significantly reduced sensitivity to both molecules compared to strain S755. As azole fungicides and lipopeptides do not have the same mode of action, the objectives of the present study were to characterise the mechanisms of reduced sensitivity to azoles and fengycin in Rs552 and to verify whether there are common mechanisms involved in this reduction in sensitivity. In total, the antifungal activities of five lipopeptides and three binary mixtures, as well as two azoles, were tested against the two *V. inaequalis* strains Rs552 and S755. The effects of the fengycin lipopeptide on the morphology and structure of the mycelium were observed using light and transmission electron microscopy. In addition, the two strains were characterised for three mechanisms involved in reduced sensitivity to azoles, including mutations in the *Cyp51A* gene, increased expression of the *Cyp51A* gene and overactivity of the efflux pump, using biochemical, molecular and bioinformatics tools to elucidate the mechanisms of the reduced sensitivity of Rs552. Finally, a lipidomic analysis was carried out to determine whether resistance to azoles and fengycin is linked to fungal lipid composition.

2. Materials and methods

2.1. Fungal strains and culture conditions

Two strains of *V. inaequalis* were provided by the IRHS laboratory, INRA Angers, France, including S755, sensitive to tebuconazole, and Rs552, with reduced sensitivity to tebuconazole, as described by Muchembled et al. (2018). Solid culture of *V. inaequalis* was performed on Petri dishes supplemented with sterile malt agar medium containing 33.6 g/L malt agar extract and 2 g/L agar, while liquid culture of the fungus was performed in Erlenmeyer flasks supplemented with sterile glucose-peptone medium at pH 6.5, containing 14.3 g/L glucose and 7.1 g/L bactopeptone. The two fungal strains were grown on solid malt agar medium in the dark at 20°C for 14 days, followed by six days under UV light (Wood light) at 20°C in order to induce fungal sporulation. These incubation conditions were applied for all experiments except the DNA extraction assay, for which incubation was undertaken for 20 days in the dark at 20°C. Spores suspensions at 10^5 spores/mL were used for other experiments. These were obtained by scraping Petri dishes with glucose-peptone medium, then collecting the supernatant by filtration. For the antifungal activity and microscopy tests, the spore suspension was used directly in the microplates. For the RNA and lipidomics experiments, the suspension was first inoculated into 250 mL Erlenmeyer flasks (90 mL medium and 10 mL spore suspension). The Erlenmeyer flasks were then incubated in the dark at 20°C and 140 rpm for 20 days (for RNA extraction) or 26 days (for lipidomic analysis). The pellets were rinsed three times with sterile water and then collected by filtration on Büchner with Whatman® filter paper. The pellets were then recovered and immersed in liquid nitrogen. For RNA extraction, the fungal biomass was shredded and stored at −20°C, while for lipid extraction, the biomass was freeze-dried.

Genome of both strains were sequenced with 39x mean coverage. Draft genomes are composed of 4132 contigs for *V. inaequalis* S755 strain and 10001 contigs for *V. inaequalis* Rs552 strains with total sequence size of 64036957 pb and 57073897 pb respectively and GC content of 43.46 % and 44.14 % respectively. Assemblage statistics L50 and N50 are 509 and 37094 respectively for S755 strain and 1870 and 8804 respectively for Rs552 strain. Sequences of draft genomes were submitted to NCBI database with accession number JBBYAA000000000 (S755) and JBBXZZ000000000 (Rs552). Genomes size and GC content are highly similar to *V. inaequalis* strains genome parameters. Alignment of the draft genomes was carried out using Jspecies software (Richter

et al., 2016) and revealed that these two strains share 98 % average nucleotide identity, with a bit score distribution of 1668 (Fig. S1).

2.2. Production, purification, structural confirmation and quantification of lipopeptides

A total of five lipopeptides were used in this study, including fengycin (plipastatin), mycosubtilin, iturin A, lichenysin and pumilacidin. These lipopeptides were solubilised in 100 % dimethyl sulfoxide (DMSO, Sigma-Aldrich, Saint-Quentin-Fallavier, France) at 60 mg/mL. The two genetically modified single-producer *Bacillus subtilis* strains Bs2504 and LBS1 were used to produce fengycin and mycosubtilin, respectively. The strain Bs2504 is derived from the strain 168 which is well known to possess a plipastatin production cluster. The production, purification and quantification of fengycin was carried out as described recently by Vassaux et al. (2021). Mycosubtilin was produced, purified, and kindly provided by Lipofabrik (Lesquin, France). The bacteria *B. velezensis* GA1, *B. licheniformis* BBG146–2, and *B. pumilus* QST 2808 were used to produce the lipopeptides iturin A, lichenysin and pumilacidin, respectively. These three bacteria were grown in lysogenic broth (LB) medium (10 g/L NaCl, 5 g/L yeast extract and 10 g/L tryptone) at 37°C and 160 rpm overnight. In addition, the Landy medium was inoculated with these bacteria at an optical density of 0.1 at 600 nm in a flask filled to 10 %. The Landy medium used for lichenysin production was modified by replacing glucose with 10 g/L xylose and 5 g/L sucrose. The inoculated flasks were then incubated at 37°C at 160 rpm for 48 h for *B. velezensis* GA1, and at 30°C at 160 rpm for 72 h for *B. licheniformis* BBG 146–2 and *B. pumilus* QST 2808.

Purification of lichenysin, pumilacidin and iturin A began with the harvesting of bacterial cells by centrifugation at 25,000 g for 30 minutes at 4°C. The resulting supernatant was acidified to pH 2 with H_2SO_4 and incubated overnight at 4°C. The acidified supernatant was then centrifuged. The pellet was resuspended in H_2O and brought to pH 8 with NaOH. Liquid-liquid extraction was carried out using the same volume of a 7:3 ethyl acetate/butanol solvent mixture. The solvent phase was dried with a SpeedDry RVC 2–25 CD Plus (Martin Christ, Germany) to a volume of 5 mL. Lipopeptide purification was carried out using PuriFlash PF4250–250 preparative HPLC (Interchim, France). The gradients used for purification were acetonitrile (ACN) in water acidified with 0.1 % (V/V) trifluoroacetic acid (TFA). For iturin A, the gradient used was: 15 min at 20 % acetonitrile (ACN), 15–35 min at 30 % ACN, 35–55 min at 50 % ACN, 55–95 min at 80 % ACN, 95–105 min at 100 % ACN and 105–125 min at 80 % ACN. For lichenysin, the gradient used was: 10 min at 70 % ACN, 10–70 min at 90 % ACN, 70–80 min at 100 % ACN and 80–90 min at 90 % ACN. For pumilacidin, the gradient used was: 15 min at 60 % ACN, 15–65 min at 85 % ACN, 65–85 min at 100 % ACN and 85–95 min at 85 % ACN. Fractions containing only pure iturin A, lichenysin or pumilacidin were pooled and concentrated using a SpeedDry RVC 2–25 CD Plus before freeze-drying with Alpha 3–4 LSCbasic (Martin Christ, Germany).

Fengycin (plipastatin) and mycosubtilin were characterised by reverse phase-high pressure liquid chromatography (RP-HPLC) using an Acquity H-Class (Waters, Massachussetts, USA) coupled with a photodiode array (PDA) and an Acquity QDa mass spectrometer (Waters), as reported in Dussert et al. (2022), while Iturin A, lichenysin, and pumilacidin were analysed as described below. Ultra-performance liquid chromatography-mass spectrometry (UPLC-MS) was used to detect lipopeptides and confirm their mass, using an Acquity UPLC H-Class sample manager with a quaternary solvent manager and SQ detector (Waters, USA). Ten μL of sample was injected onto a Waters Acquity BEH C18 1.7 μm column (2.1×50 mm) with a C18 1.7 μm precolumn. The flow rate and temperature were set at 0.6 mL/min and 40°C. The gradient of ACN in water acidified with 0.1 % (V/V) TFA was as follows: from 30 % ACN to 95 % ACN in 2.43 min, maintained at 95 % ACN until 5.10 min, from 95 % ACN to 30 % ACN in 0.1 min and maintained at 30 % ACN until the end of the run (7 min). Detection was carried out by electrospray in positive ion mode, using the following parameters: source temperature 130°C, desolvation temperature 400°C, nitrogen flow rate 1000 L/h and cone voltage 120 V. Data acquisition and processing were carried out using MassLynx, version 4.1.

For quantification, a Nexera ultra-high performance liquid chromatography with diode array detection UPLC-DAD (Shimadzu, Japan) was used with the same column, mobile phase and run parameters as the UPLC-MS used. The analysis spectrum used by the DAD was between 190 and 800 nm. A calibration curve for an external surfactin standard (Kaneka, Japan) and a fengycin or mycosubtilin standard (Lipofabrik, France) was used to compare the surface area of the surfactin, fengycin and iturin A molecules obtained. The purity of the molecules obtained was 98 % for fengycin, 75 % for mycosubtilin, 97 % for iturin A, 98.5 % for lichenysin and 77 % for pumilacidin.

2.3. Biological tests on antifungal activity and efflux pump modulators

Tebuconazole, tetraconazole (triazole), tolnaftate (thiocarbamate) and three efflux pump modulators (EPMs) (amitriptyline hydrochloride, chlorpromazine hydrochloride and verapamil hydrochloride), purchased from Sigma-Aldrich (Sigma-Aldrich, France), were used in the present study. These molecules were solubilised in 100 % DMSO at 40 mg/mL for the fungicides and 50 mg/mL for the EPMs.

The antifungal activity of five lipopeptides (fengycin, mycosubtilin, iturin A, lichenysin and pumilacidin) and three binary mixtures (50/50, w/w) (fengycin/iturin A, fengycin/lichenysin and fengycin/pumilacidin), two azoles (tebuconazole and tetraconazole) and tolnaftate were evaluated against the two strains of *V. inaequalis* S755 *and* Rs552 using 96-well microplates in glucose-peptone liquid medium, as described in Desmyttere et al. (2019). A total of 15 concentrations were used for the lipopeptides evaluated (0.0026, 0.0051, 0.010, 0.021, 0.041, 0.082, 0.164, 0.328, 0.656, 1.31, 2.63, 5.25, 10.5, 21 and 42 mg/L) and fungicides (0.0017, 0.0034, 0.0068, 0.014, 0.027, 0.055, 0.109, 0.219, 0.438, 0.875, 1.75, 3.5, 7, 14 and 28 mg/L), as well as controls with no compound. The experiment was repeated three times independently, with four biological replicates in each experiment.

For the efflux pump bioassays, two concentrations of EPMs without significant antifungal activity were used (4.5 and 7 mg/L). Tebuconazole, fengycin and tolnaftate were tested in combination with EPMs. Due to the different sensitivities of the two strains to tebuconazole (and other fungicides), six concentrations per fungicide were tested, including three concentrations close to the IC_{50} of each strain, on both strains. The EPMs bioassays were carried out in liquid glucose-peptone medium in 96-well microplates. The EPMs were first mixed with the glucose-peptone medium, then each fungicide was added at specific concentrations. After six days of incubation, optical density values were recorded. The experiment was repeated three times independently, with six biological replicates in each experiment.

Interactions between EPMs and fungicides were analysed according to Colby (1967) by calculating the expected growth of the mixtures ($Exp = X_F.X_M/100$), where X_F and X_M represent the percentage growth of the control for the fungicide and the EPM, respectively. Observed growth (Obs) is the percentage growth of the control for the mixtures. Interaction was determined by the ratio IR=Exp/Obs. The interaction between fungicides and EPMs was considered additive when $0.5<IR<1.5$, synergistic when $IR\geq1.5$, or antagonistic when $IR\leq0.5$ (Leroux and Walker, 2013).

2.4. Microscopic observations

The effect of fengycin on the mycelial morphology of both *V. inaequalis* strains S755 and Rs552 was assessed using light microscopy and transmission electron microscopy (TEM). Observations were made on samples of fungal mycelium taken from 96-well microplates supplemented with liquid glucose peptone medium and incubated for six days, prepared as described above. Three concentrations of fengycin

were observed by light microscopy, namely 0.021 mg/L, 0.66 mg/L and 42 mg/L (corresponding respectively to the concentration around S755 IC_{50}; an average concentration and the highest concentration tested). The last two concentrations were also used for TEM observations. In total, three samples were taken per concentration for each strain and compared with untreated controls. For light microscopy, microscope slides were prepared by depositing five μL of lactophenol blue with five μL of each fungal culture containing the mycelium, before being observed under a Nikon Eclipse 80i microscope supplemented by a Nikon Ddxm1200c digital camera. TEM observations were performed by fixing the contents of the microplate wells for 2 h, rinsing in 0.2 M cacodylate buffer, and postfixing for 1 h in 1 % osmium tetroxide (OsO_4) in 0.1 M cacodylate buffer, followed by rinsing in MilliQ water. The bottom of the plate wells was then scraped with a metal spatula to suspend the contents. The contents were collected using a glass pipette and transferred to Eppendorf tubes. The samples were dehydrated in a series of ethanol, then acetone, before being embedded in AGAR 100 epoxy resin. The samples were centrifuged to decant between bath changes. The resin blocks at the bottom of the Eppendorf tubes were removed from the moulds and sawed into two parts, then reintegrated into the resin in flat silicone moulds. The resin capsules were then cut using a diamond knife mounted on a Sorvall Porter-blum MT2 B ultramicrotome. Ultrathin sections were cut at 80–100 nm and contrasted with Uranyless (Deltamicrocopies, Mauressac, France) for TEM observation (STEM Tecnai G2 twin operating at an accelerating voltage of 160 kV).

2.5. DNA extraction, PCR amplification and Sanger sequencing of the *Cyp51A* gene

DNA from both *V. inaequalis* strains S755 and Rs552 was extracted for whole genome sequencing and *Cyp51A* gene analyses. DNA was extracted from fungal strains grown on solid malt agar medium. The mycelium was scraped, frozen in liquid nitrogen and ground using a mortar and pestle. Eighty mg of fungal powder was resuspended in 300 μL of PPI water and sonicated for 20 minutes. DNA was extracted using a phenol/chloroform extraction method described previously (Siah et al., 2010) with volumes doubled in order to obtain sufficient quantities of DNA for all analyses.

The *Cyp51A* gene and its putative promoter (upstream region) were amplified using the primers described in Table S1. PCR reactions were performed using the following mixture: 0.2 μL (20 μM) of each primer, 4 μL of dNTP (2.5 mM), 5 μL of 10 X reaction buffer, 8 μL (25 mM) of MgCl2, 0.25 U of Taq polymerase (Fisher BioReagents™) and 5 μL (1 ng/μL) of genomic DNA, all adjusted to a volume of 50 μL with PPI water. PCR amplifications were performed in the Bio-Rad C1000 Touch thermal cycler (Bio-Rad Laboratories Inc.) with the following thermal cycling conditions: 2 min at 95°C; 30 cycles of 30 s at 94°C, 30 s at 57.5°C (*Cyp51A* gene) or 55.2°C (upstream region) and 1 min at 72°C; followed by a final elongation of 10 min at 72°C.

The amplicons obtained were sequenced by Genoscreen (Lille, France) using the Sanger method. A 1674 bp fragment of the *Cyp51A* coding sequence was concatenated by superimposing the amplified fragments using the BLASTn alignment search tool (blast.ncbi.nlm.nih.gov/Blast.cgi). Sequences from the upstream region of *Cyp51A* from both strains were also aligned using BLASTn. Nucleotide and amino acid sequences were aligned using Clustal Omega (ebi.ac.uk/Tools/msa/clustalo). The resulting sequences were compared using Clustal Omega to the sequences of the myclobutanil (azole)-resistant strain Ent54 (ACC#AF262756) and the myclobutanil-sensitive strain Ent27 (ACC#AF227920), both reported by Schnabel and Jones (2001). These sequences were aligned using Clustal Omega with the sequences of the Ent54 and Ent27 strains. In addition, the final sequences obtained from the upstream region were aligned with the sequence of the sensitive strain 3a-27–10 (ACC#KT694303) reported by Villani et al. (2016).The GenBank accession numbers for nucleotide sequences are BankIt2770571 755_CYP51 OR909969 for S755 strain and BankIt2770571 552_CYP51 OR909970 for Rs552 strain.

2.6. Docking and dynamics of the CYP51A protein

In silico dynamic and docking analyses were performed to assess the effect of the S183C substitution detected (in the CYP51A protein of the sensitive *V. inaequalis* strain S755) on affinity with the fungicide tebuconazole. We chose to build a putative structure by homology, in the absence of an experimental 3D structure of CYP51A from *V. inaequalis*. A BLAST on the RCSB Protein DataBank (PDB) retrieved a number of structures, from which we retained the four with the highest sequence identity for further evaluation, all of which were within a reasonable 47.5 %. A thorough inspection of the alignment was carried out to validate the choice of reference by closely monitoring the heme-binding residues. Mutants were obtained by mutating the corresponding residue in the *V. inaequalis* model. After assessing their potential effect on structure, a series of inhibitors were docked to GOLD (Jones et al., 1995) and the binding site was defined as an 8 Å sphere around the tebuconazole position extracted from 5eac. Thirty poses were generated and their superposition in well-defined groups allowed us to determine the pose to be retained as the final solution. Another criterion was the score of the pose most representative of the clusters. To better understand the effect of strain S755 substitution, a 100 ns molecular dynamics run was performed in quadruplicate with the AMBER package (Case et al., 2019) and the difference in interactions between strains S755 and Rs552 was assessed using Structural Interaction Network Analysis Protocols (SINAPs) (Bedart et al., 2022).

2.7. Illumina whole genome sequencing and bioinformatics mapping of *Cyp51A* transcription factors and efflux pump genes

Whole DNA from both *V. inaequalis* strains was sequenced at MicrobesNG (microbesng.com) using Illumina MiSeq and HiSeq 2500 technology platforms, with paired-end reads ranging from 2 to 250 bp. The closest existing reference genome was determined using Kraken (Wood and Salzberg, 2014) and reads were mapped using the burrows-wheeler aligner (BWA) MEM algorithm (bio-bwa.sourceforge.net) to assess data quality. Reads were assembled *de novo* using SPAdes (cab.spbu.ru/software/spades).

Based on the Sanger sequences, transcription factor binding motifs in the upstream region of *Cyp51A* from the two *V. inaequalis* strains were identified using Multiple Em for Motif Elicitation Suite version 5.3.3 (MEME Suite) (Bailey and Elkan, 1994). The first analysis revealed motifs in the promoter sequences, using MEME and the motif alignment and search tool (MAST) with the following parameters: motif width of 6–15 bp, zoop pattern and classical mode. In addition, all motifs found were analysed using the Gene Ontology for Motifs (GOMo) (Buske et al., 2010) in order to determine or suggest a biological role. In addition to the bioinformatics analyses performed to detect transcription factor binding motifs, a review of the scientific literature was used to find previously identified motifs (Fig. 4E). By using MAST to align motifs, it was possible to identify motifs with a known biological role. On the basis of the whole genome sequences obtained, the *ABC* and *MFS* efflux pump gene sequences were mapped on the draft genome of each strain using a local blast. Sequence variations in the target genes were identified by alignment using Clustal Omega.

The GenBank accession numbers for nucleotide sequences are BankIt2770571 755_MFS1 OR909971, BankIt2770571 552_MFS1 OR909972, BankIt2770571 755_ABC1 OR909973, BankIt2770571 552_ABC1 OR909974, BankIt2770571 755_ABC2 OR909975, BankIt2770571 552_ABC2 OR909976, BankIt2770571 755_ABC3 OR909977, BankIt2770571 552_ABC3 OR909978, BankIt2770571 755_ABC4 OR909979, BankIt2770571 552_ABC4 OR909980.

2.8. RNA extraction and analysis of relative Cyp51A gene expression by RT-qPCR

Cyp51A gene expression in both strains was assessed after 20 days of fungal incubation in liquid medium, in the absence and presence of tebuconazole or fengycin at the same concentrations for each inhibitor (Rs552, 0.4 mg/L; S755, 0.005 mg/L). RNA was extracted from the ground (mortar and pestle) and stored biomass of the two *V. inaequalis* strains. For each extraction, 80 mg of pellet powder was used. Extraction was performed using the RNeasy Mini kit (Qiagen, Hilden, Germany) with DNase treatment (ThermoFisher Scientific, Waltham, Massachusetts, USA). RNA concentration was measured using a nanodrop. RNA quality was assessed using a 1.5 % agarose gel in 1 X TAE to check RNA integrity.

To determine the relative expression of *Cyp51A*, cDNA synthesis was performed using the iScriptTM Reverse Transcription Supermix for RT-qPCR (Biorad Laboratories, Hercules, California, USA). Reverse transcription was performed in a mixture containing 4 µL RT, 10 µL 100 ng/µl RNA and 6 µL ultrapure water, under the following conditions: 5 min at 25°C, 20 min at 46°C and 1 min at 95°C. Freshly synthesised cDNAs were diluted by half and stored at −20°C.

Quantitative polymerase chain reaction (qPCR) was performed with a pair of primers targeting *Cyp51A* and also with two pairs of primers targeting the *GAPDH* and *actin* housekeeping genes (Table S1). Reactions were carried out in a final volume of 10 µL: 5 µL of SYBR Green (iTaq Universal SYBR Green supermi; Biorad Laboratories, Hercules, California, USA), 1 µL of 5 µM primers, 2 µL of ultrapure water and 2 µL of cDNA. Amplifications were monitored using the Bio-Rad CFX96 real-time PCR detection system (Bio-Rad Laboratories Inc.) with the following thermal profile: 3 min at 95°C, (15 sec at 95°C, 30 sec at 60°C) x 39 cycle, 30 sec at 65°C, and 30 sec at 95°C for amplicon dissociation curves.

A primer validation experiment was carried out beforehand. To determine the relative expression of *Cyp51A*, the comparative threshold cycle (Ct) method (Schmittgen and Livak, 2008) was used using formula $2^{-\Delta\Delta Ct}$. The control sample was the sensitive strain S755 in the absence of fungicide to determine expression. Three biological replicates with three technical replicates per biological replicate were performed for each modality.

2.9. Lipid extraction and analysis

Sterols were identified and quantified from 50 mg of freeze-dried mycelium. Direct saponification was carried out with the addition of an internal standard (cholesterol) and 3 mL of methanolic potash. The whole was placed on a heating block for 2 hours at 70°C. The sterols were then extracted by adding 5 mL of hexane and 1 mL of water, then homogenised using a vortex. The upper phase was recovered and placed in another tube. The addition of hexane, homogenisation and recovery of the upper phase were repeated twice. The upper phase was concentrated under vacuum in a centrifugal evaporator, the sterols were extracted into 2 mL of hexane and placed in a flask, then concentrated in a centrifugal evaporator. The sterols were recovered in 200 µL of hexane. The sterols were analysed using a Shimadzu QP-2010 Ultra gas chromatograph-mass spectrometer (GC-MS) (Shimadzu, Japan) equipped with a single quadrupole mass detector and simultaneously coupled to a flame ionisation detector (FID). Samples were analysed in fractionated mode (80:1 ratio) on a ZB-5MS fast capillary column (10 m length x 0.1 mm internal diameter x 0.1 µm phase thickness, 5 % phenylarylene / 95 % dimethylpolysiloxane, Zebron, Phenomenex, Torrance Calif, U.S.A.) using helium as the carrier gas at a constant linear velocity (50 cm/sec). The injector temperature was 280°C and the detector temperature was 380°C and 280°C for the FID and ion source, respectively. The temperature programme started with an initial temperature of 130°C and increased by 50°C every minute to reach a final temperature of 330°C, which was maintained for 2 minutes. The ionisation mode was electron impact at 70 eV and the mass range between 50.0 and 600.0 u was scanned. SIM (single impact monitoring) mode was used simultaneously. Sterol quantification was performed using cholesterol (Sigma-Aldrich) as an internal standard. Sterols were identified by comparing their relative retention times with those of commercial sterol standards (Sigma-Aldrich) and by comparing them with spectra obtained from commercial standards and/or published in the literature (NIST standard reference database). Three biological replicates with five technical replicates per biological replicate were carried out for each modality.

Phospholipids were extracted and analysed by Lipometrix (Leuven, Belgium) (Talebi et al., 2023). These analyses were carried out using approximately 10 mg of freeze-dried mycelium from two different strains of *V. inaequalis*. Briefly, the *V. inaequalis* pellets were homogenised in water, then the lipids and internal standard were extracted with 1 N HCl:CH_3OH 1:8 (v/v), $CHCl_3$ and 200 µg/mL antioxidants. The organic phase was recovered and evaporated. The pellet was solubilised in ethanol and analysed by liquid chromatography tandem mass spectrometry with electrospray ionisation. The negative ionisation mode using fatty acid fragment ions was used to measure phospholipids. Peaks were integrated using MultiQuant software™. Isotopic contributions were used to correct lipid species signals. Finally, quantification was carried out in accordance with Lipidomics Standard Initiative (LSI) guidelines. Three biological replicates were performed for each modality.

2.10. Statistical analysis

A half-maximal inhibitory concentration (IC_{50}) was calculated from the dose-response curve obtained for each lipopeptide or fungicide and for each fungal strain, using non-linear regression completed in XLSTAT software (Lumivero, France). The comparison of IC_{50} values between molecules and strains was carried out using a one-way ANOVA followed by a Tukey test with a global α risk of 5 %, using XLSTAT software. For the gene expression assay, statistical analyses were performed on the $2^{-\Delta\Delta Ct}$ values using a one-way ANOVA followed by a Tukey test with a global α risk of 5 %, using XLSTAT software. The relative composition of sterols and phospholipids was analysed. All compounds representing less than 1 % were excluded from the statistical analysis. The conditions of use (normality and homoscedasticity) were checked and validated. Based on the relative compositions, a one-way ANOVA followed by a Tukey test was performed to determine whether there was a significant difference between the two strains. The p-values were compared with an adjusted α-risk (Bonferroni adjustment) by dividing the global α-risk of 0.05 by the maximum number of molecules tested (0.05/7=0.007 for seven molecules, for example).

3. Results

3.1. Lipopeptide characterisation using RP-HPLC-MS

The lipopeptides used in the present study were first characterised with RP-HPLC-MS (Fig. S2 A-E). Analysis of lichenysin revealed the presence of four major isoforms with a C13 to C15 fatty acid chain, the amino acid in position 7 being either Valine or Leucine (*m/z* [M+Na+] 1030, 1029, 1044, respectively). Analysis of pumilacidin showed the presence of six major isoforms with a fatty acid chain from C15 to C17 but also changes in position 7 of the peptidic chain, which can be either a leucine or a valine (*m/z* [M+Na+] 1059, 1073, 1087 and 1101, respectively). Analysis of iturin A reveals the occurrence of three major isoforms displaying a fatty acid chain from C14 to C16 (*m/z* [M+Na+] 1065, 1079 and 1093, respectively). Analysis of mycosubtilin solution highlighted the presence of five major isoforms containing a fatty chain from C14 to C18 (*m/z* ([M+H]+ 1043, 1057, 1071 and 1099, respectively). Finally, the analysis of fengycin (plipastatin) showed the presence of 9 major isoforms of plipastatin A or plipastatin B containing a

fatty chain from C15 to C19 (*m/z* ([M+H+H]+ 725, 732, 739, 746, 731, 753, 738, 760 and 745, respectively).

3.2. The Rs552 strain showed reduced sensitivity to azoles and fengycin, but not to other lipopeptides

The antifungal activity of five lipopeptides (alone or in a binary mixture) and two azole active substances was evaluated against the two *V. inaequalis* strains S755 and Rs552 (Fig. 1A; Table S2). As expected, the two strains showed distinct levels of sensitivity to tebuconazole (IC_{50} values of 0.012 and 1.153 mg/L for S755 and Rs552, respectively), confirming previous results (Desmyttere et al., 2019). The two strains also showed distinct levels of sensitivity to tetraconazole (IC_{50} values of 0.009 and 0.907 mg/L for S755 and Rs552, respectively). The IC_{50} values and the sensitivity patterns of both strains S755 and Rs552 to tebuconazole are close to those highlighted in a preliminary experiment on solid medium for two reference *V. inaequalis* field strains (NRRL 66904, baseline sensitive isolate and NRRL 66905, a DMI resistant isolate) previously assessed by Lichtner et al. (2020), with a resistant factor (ratio IC_{50} of resistant *versus* IC_{50} of sensitive) of 61 for both couples of strains S755-Rs552 and NRRL 66904-NRRL 66905 (*data not shown*).

With an IC_{50} value of 0.024 mg/L for S755, fengycin showed strong activity, close to that of tebuconazole. It is interesting to note that fengycin showed an IC_{50} value greater than 42 mg/L for Rs552. Mycosubtilin was the second most active lipopeptide, while iturin A was the third. These two compounds from the iturin family showed the same level of activity on both strains, with mycosubtilin being more active than iturin A. Lichenysin and pumilacidin from the surfactin family showed an IC_{50} value greater than 42 mg/L on both strains.

For the FI binary mixture, the activity was higher for strain S755 than for strain Rs552. For strain S755, the activity was intermediate between that of fengycin alone and that of iturin alone. For strain Rs552, the activity was equal to that of iturin alone and identical to that of the azoles. For the FL and FP binary mixtures, the activities were also higher for strain S755 than for strain Rs552. For strain S755, the activity was similar to that of fengycin alone. Surprisingly, activities were calculated for Rs552, while fengycin, pumilacidin and lichenysin alone had no activity.

Analysis of the chemical structure of lipopeptides has shown that they are made up of a peptide part and a fatty acid chain of variable nature. Fengycin is the only decapeptide tested, while the other lipopeptides are heptapeptides. Similarly, the length of the fatty acid chains varies from C12 to C17 depending on the lipopeptides tested and there are several possible isoforms per lipopeptide (Fig. 1B). Although the activities of the heptapeptides are identical in the 2 strains, they are very different in structure. Iturin A showed good activity but was statistically weaker than mycosubtilin. We found that iturin A differed from mycosubtilin only by the inversion of Ser and Asn in positions 6 and 7 of the peptide part and by a shorter fatty acid chain. Similarly, pumilacidin and lichenysin do not have the same amino acid nature and fatty acid chain length as iturin A and mycosubtilin.

3.3. Fengycin induces morphological and cytological changes

Light microscopic observations were performed to determine whether morphological changes in the mycelium of the two strains of *V. inaequalis* occur in the presence of fengycin. In the control condition, the mycelium was well developed with long and regular hyphae (Fig. S3A, B). Vesicle-like structures, which formed a sac that could be slightly swollen or cracked, were observed in both strains (Fig. S3C, D, E, F), hence agreeing previous results (Desmyttere et al., 2019). These vesicle-like structures were observed in relation to the concentration and with a greater presence in strain S755 compared to strain Rs552 (*data not shown*). To investigate these changes further, TEM observations were made on the mycelium of both strains grown in the presence of fengycin and compared with untreated fungal mycelium. Under control conditions, the cell walls and plasma membrane were uniform and intact (Fig. 2A, B). In the presence of fengycin, the plasma membrane became incomplete, and the cytoplasmic content was reduced, becoming more transparent and less abundant, or even partially lost (Fig. 2C, D). Vesicle-like structures appeared to be formed by an empty space between two cell walls (Fig. 2E, F). These observations point to a mode of action involving modifications of the fungal cell wall, plasma membrane and cytoplasm compromising cellular integrity, with a lower abundance of vesicles in Rs552 compared to S755.

3.4. S183C substitution in CYP51A with no effect on azole affinity

In order to identify the mechanisms responsible for the difference in sensitivity to tebuconazole, the *Cyp51A* gene (encoding the CYP51A enzyme, the target of azoles) of the two *V. inaequalis* strains S755 (ACC#OR909969) and Rs552 (ACC#OR909970) was sequenced in its entirety (1674 bp). Comparison of the sequences obtained from S755 and Rs552 with those of the *Cyp51A* gene from two strains in the literature (Ent27 and Ent54, respectively sensitive and resistant to myclobutanil (Schnabel and Jones, 2001) revealed a non-silent mutation in sensitive strain S755 at position 710 bp (Fig. 3A). Strain S755 had a thymine, while Ent54, Ent27 and Rs552 had an adenine. This mutation resulted in a change in amino acid sequence, corresponding to the substitution of a serine for a cysteine at position 183 (S183C) in strain S755 (Fig. 3B). Serine and cysteine are uncharged polar amino acids, but

(A)

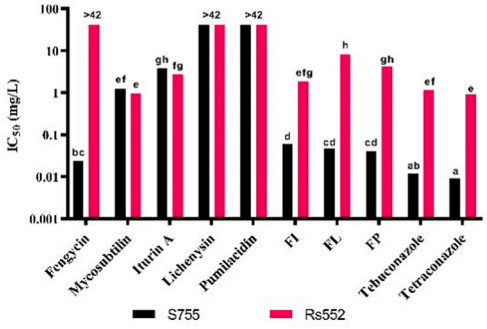

(B)

Lipopeptide	Peptide moiety										Main fatty acid chains	Reference
Position of amino acid	1	2	3	4	5	6	7	8	9	10		
Fengycin	L-Glu	D-Orn	D-Tyr	D-aThr	L-Glu	D-Ala or D-Val	L-Pro	L-Gln	L-Tyr	L-Ile	C15, C16 or C17	Jacques, 2011
Mycosubtilin	L-Asn	D-Tyr	D-Asn	L-Gln	L-Pro	D-Ser	L-Asn				C16 or C17	Jacques, 2011
Iturin A	L-Asn	D-Tyr	D-Asn	L-Gln	L-Pro	D-Asn	L-Ser				C14 or C15	This study
Pumilacidin	L-Glu	L-Leu	D-Leu	L-Leu	L-Asp	D-Leu	L-Val or L-Leu				C15, C16 or C17	This study
Lichenysin	L-Gln	L-Leu	D-Leu	L-Val	L-Asp	D-Leu	L-Val or L-Leu				C12, C13, C14, C15 or C16	This study

Fig. 1. Lipopeptide analysis and antifungal activity against the two *V. inaequalis* strains S755 and Rs552. **A**, Antifungal activity of five lipopeptides (fengycin, mycosubtilin, iturin A, surfactin, lichenysin, pumilacidin), three binary mixtures of them (fengycin-iturin A, fengycin-lichenysin, fengycin- pumilacidin), and two azole fungicides (tebuconazole and tetraconazole) against S755 and Rs552. Bars with different letters indicates a significant difference according to ANOVA-Tukey test at α=0.05. **B**, Molecular structures of the assessed lipopeptides, with a description of the peptide moiety and the fatty acid chain.

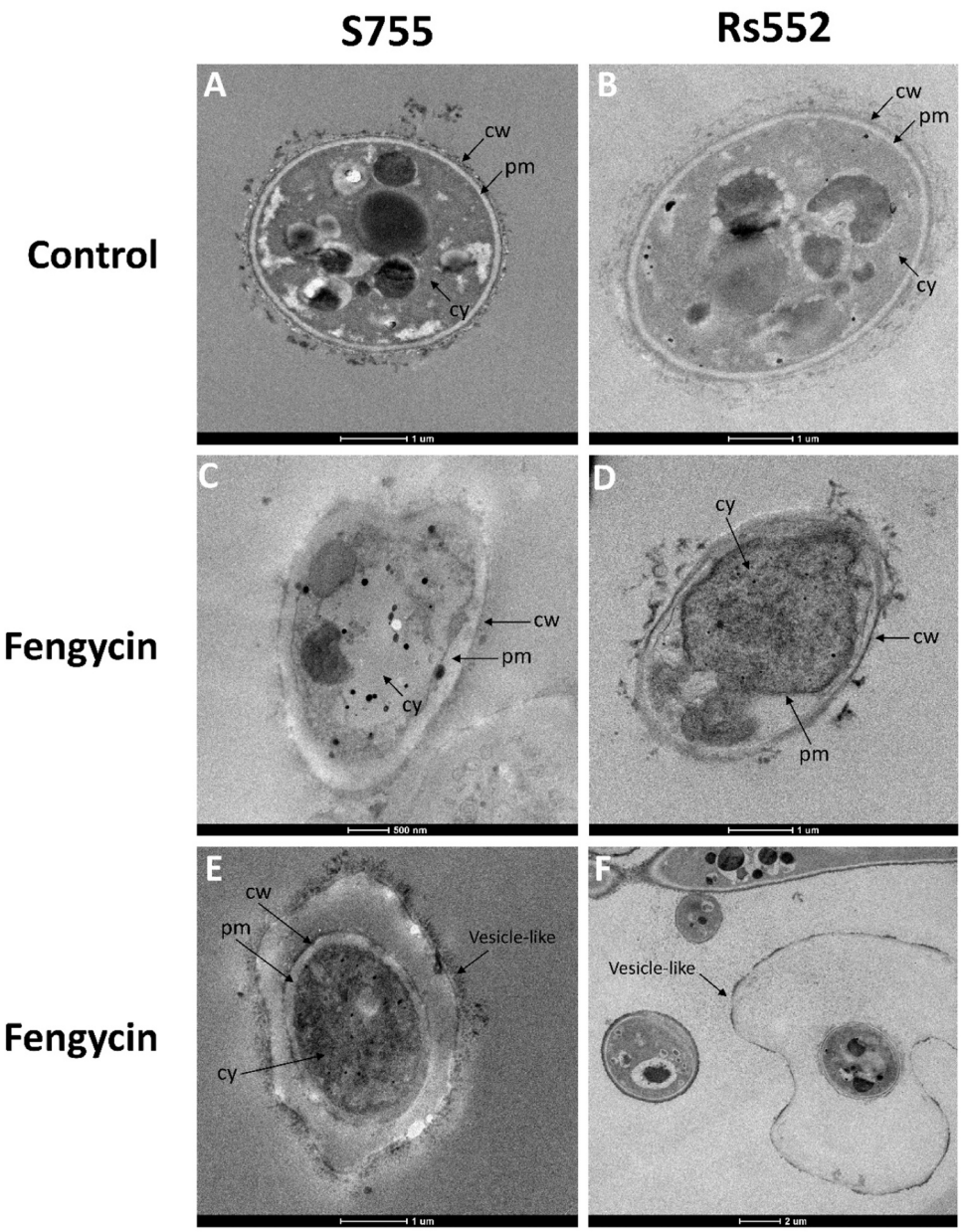

Fig. 2. Observations of the mycelium of both *V. inaequalis* strains S755 and Rs552 using transmission electron microscopy; **A**, S755 control; **B**, Rs552 control; **C**, S755 at 0.66 mg/L fengycin; **D**, Rs552 at 0.66 mg/L fengycin; **E**, S755 at 0.66 mg/L fengycin; **F**, Rs552 at 42 mg/L fengycin. cw, cell wall; pm, plasma membrane; cy, cytoplasm.

cysteine is a sulphur amino acid that can form disulfide bridges in the corresponding protein.

Given that such an amino acid substitution could affect the affinity of azoles with the CYP51A enzyme, docking and dynamics analyses were carried out *in silico* to test this hypothesis. The docking of a series of several azoles (difenoconazole, epoxiconazole, metconazole, prothioconazole, tebuconazole and prochloraz) and the molecular dynamics of CYP51A of the two strains Rs552 and S755 and that of strain Ent54 taken from the literature (Schnabel and Jones, 2001) were carried out. The four structures found in the PDB database with the best sequence identity were 4lxj (*S. cerevisiae* CYP51 bound to lanosterol), 5eac (*S. cerevisiae* CYP51 bound to R-tebuconazole), 5eah (*S. cerevisiae* CYP51 bound to difenoconazole), and 4 wmz (*S. cerevisiae* CYP51 bound to fluconazole). All these models had a resolution of between 2.54 and 1.96 Å. As we were interested in the binding mode of tebuconazole, we selected 5eac as the crystallographic reference to construct a 3D model of CYP51A from *V. inaequalis* (Fig. 3C). Sequence identity is 47.5 %, which is high enough to produce a plausible model. In addition, alignment showed that the residues involved in heme group binding are conserved. There is no peptide torsion outside a 15° window around the anti-planarity and no inverted chirality. The Ramachandran plot showed that four residues (0.9 %) were in the unauthorised region.

The CYP51A sequences of S755 and Rs552 were constructed by mutating the residue corresponding to position 183 (Fig. 3D). As expected from the position of S/C183, no clear differences were found between Rs552 and S755 when docking difenoconazole, epoxiconazole, metconazole, prothioconazole, tebuconazole and prochloraz. All of them were placed close to the heme. Prothioconazole was the least effective. Its dihydrothiazole-3-thion pointed away from the heme in just under 2/3 and 1/3 of the exposures for Rs552 and S755, respectively. Difenoconazole and tebuconazole obtained the best results, with almost all of the 30 poses being superimposable on the crystallographic structure of tebuconazole.

A molecular dynamics study was carried out to investigate the effect

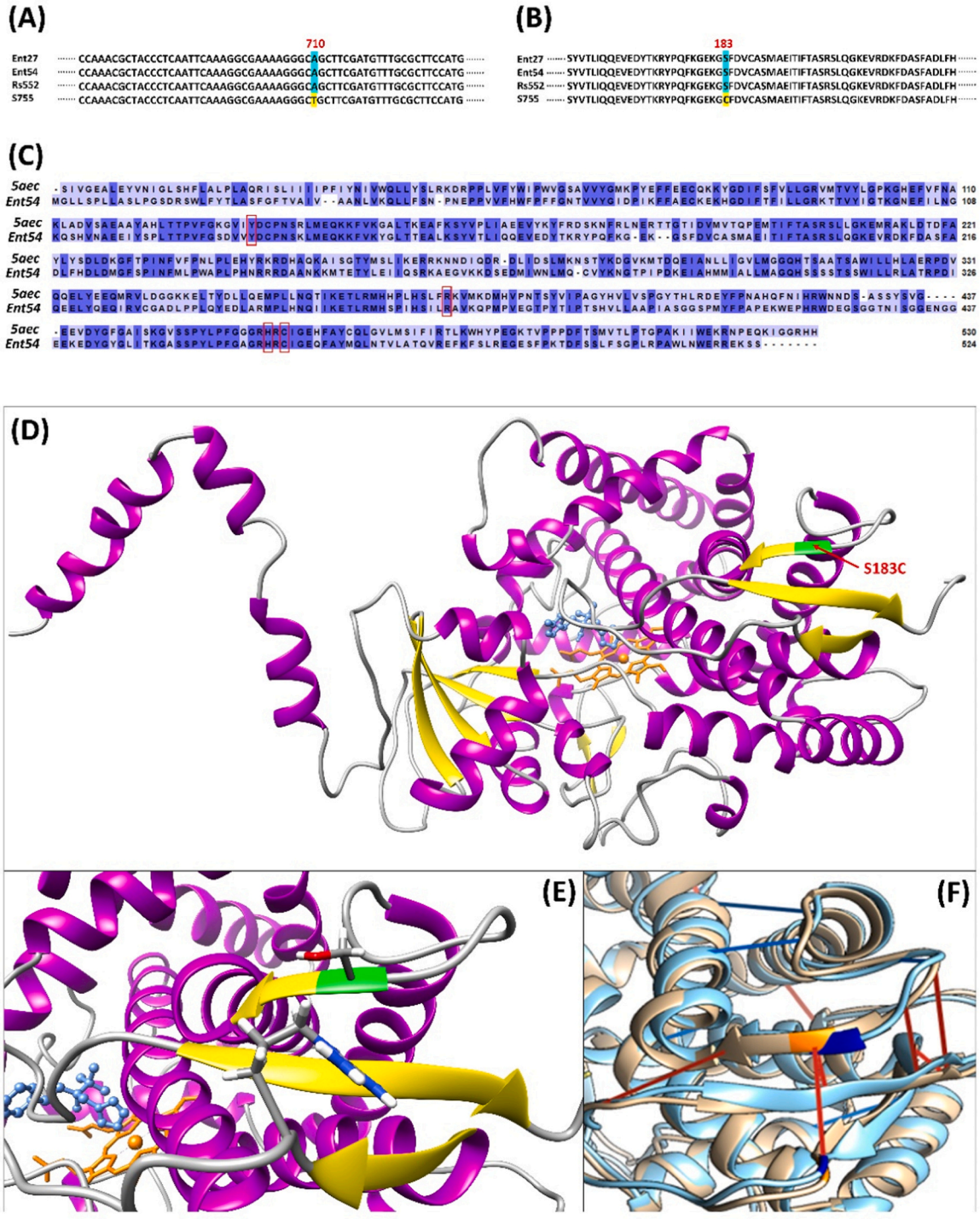

Fig. 3. Structural and *in silico* functional analysis of CYP51A in the two *V. inaequalis* strains S755 and Rs552. **A**, Alignment of the obtained *Cyp51A* nucleotide sequences. Ent27, myclobutanil sensitive strain (AAC#AF227920) (Schnabel and Jones, 2001); Ent54, myclobutanil resistant strain (ACC# AF262756) (Schnabel and Jones, 2001); Rs552, azole reduced sensitivity strain (ACC#OR909970); S755: azole sensitive strain (ACC#OR909969). **B**, Alignment of the obtained *Cyp51A* amino-acid sequences. **C**, Sequence alignment of *5eac* (*S. cerevisiae* CYP51 enzyme) and *Ent54* (*V. inaequalis* CYP51 enzyme from the strain Ent54). Residues involved in the heme binding are encased in red. **D**, Model of CYP51A in *V. inaequalis*, with position of the CYP51A S183C substitution (in green). The helices are depicted in magenta, β sheets in yellow, the heme in orange, and tebuconazole in blue. **E**, Position of Ser 183 and Cys 492 in CYP51A. **F**, Differences of interaction between the serine bearing Rs552 (red) and the cysteine bearing S755 (blue). The interactions shown are present 80 % or more of the simulation time.

of the S183C substitution in strain S755. Interestingly, Arg 492 was spatially close to 183. Positioned at the beginning of the β3 leaflet, residue 183 was followed by a loop forming a channel at the entrance to the catalytic pocket (Fig. 3E). Therefore, any change in its interaction network could have affected the stiffness or position of the loop at the entrance, which would have had a significant impact on the enzyme cycle. Four independent 100 ns dynamics were run for Rs552 and S755 CYP51A, combining the results to obtain a wider range of conformations. The interactions of residue 183 were then studied with SINAPs (Fig. 3F). Although there were no observable differences in conformation or loop plasticity, Ser 183 was consistently engaged in hydrogen bonding with Arg 492, accounting for 80 % of the simulation time,

whereas Cys 183 was notably devoid of such bonding. Overall, the substitution detected in the CYP51A S755 enzyme had no potential effect on its structure and probably on its activity.

3.5. *Rs552 constitutively displays an increased Cyp51A gene expression, probably due to variations in the promoter region and the sequence of the transcription factor*

The Rs552 strain constitutively expressed the *Cyp51A* gene 4.9 times more than the sensitive strain (Fig. 4A). Furthermore, no significant induction of the *Cyp51A* gene was observed in each strain in the presence of tebuconazole or fengycin compared with the control. These results indicate that the increased expression of *Cyp51A* is not induced by either tebuconazole or fengycin, but that the gene is constitutively more expressed in the Rs552 strain. In order to identify the potential causes of this constitutive increased expression in Rs552, additional analyses were carried out by characterising the putative promoter region of the *Cyp51A* gene in both strains, using PCR amplification and Sanger sequencing. The promoter sequences of the *Cyp51A* gene were compared between the two strains (Fig. 4B) as well as with strain 3a-27–10, which is sensitive to myclobutanil and difenoconazole (Villani et al., 2016). This comparison revealed marked variations in the region upstream of *Cyp51A*. For both strains Rs552 and S755, a 499 bp insertion was observed (in yellow) relative to 3a-27–10. For strain Rs552, in addition to the 499 bp insertion, a second 613 bp insertion (in blue) was detected twice. The first 613 bp insertion is located within the 499 bp insertion. An 18 bp deletion was also observed in Rs552 (green). In addition, two deletions were observed at positions 385 and 402 in both Rs552 and S755 compared with strain 3a-27–10 (Villani et al., 2016). The sequences of the 613 bp insertions (in blue) are identical. Our results are in agreement with previous work indicating that the *V. inaequalis* genome has a higher repetitive content than that of other fungal species, with repetitive regions occupying up to 47 % of their genome sequence (Khajuria et al., 2022).

In addition, an analysis of putative *Cyp51A* transcription factor binding motifs was performed using Illumina whole genome sequencing of both strains. Using MEME and MAST software, a total of 15 motifs were found (Fig. 4C, D). GOMo analysis was used to identify the putative biological functions of these motifs. Motif 3 showed 83 % specificity for binding to a transcription factor (ACC#GO:0003700). Among the transcription factors found, a sterol regulatory protein (UPC2) was detected. This protein is a transcription factor that binds sterol regulatory elements in *S. cerevisae* with a CGG-Nx-CCG type binding site (Marmorstein et al., 1992). In addition to the analysis of the MEME suite, a literature

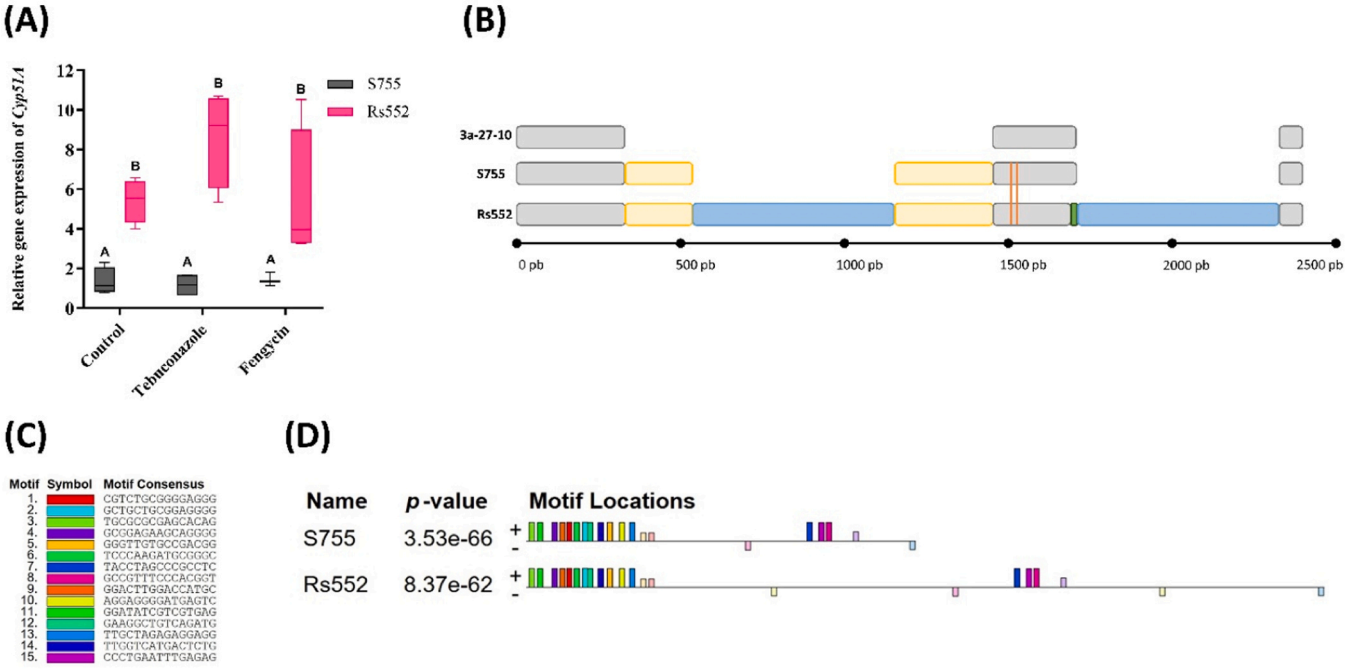

(E)

Protein	Function	Binding motif	Reference
SrbA	Transcription factor	A/T TCAC C/A CCA T/C	Blosser *et al.*, 2012
SrbA	Transcription factor	A/G TCA T/C/G C/G CCAC T/C	Chung *et al.*, 2014
Sre	Transcription factor	A/G C/T C A/G/T NN C/T C/T/G A C/T	Todd *et al.*, 2006
SrbA	Transcription factor	ATCNNNNNAT	Linde *et al.*, 2012
AtrR	Transcription factor	CGG-Nx-CCG	Hagiwara *et al.*, 2017

(F)

Binding motif	Position in S755	Position in Rs552
ATCCCAAGAT	-1010	-2217
ATCCCTGAAT	-288	-882
ATCGGTTCAT	X	-1720 and -723
CGGCAATTCCCGTGGCAACCCG	-511	-1105
CGGTGGCTCCGCCACCG	X	-1615 and -428

Fig. 4. Expression of the *Cyp51A* gene and sequence analysis of the *Cyp51A* upstream region (putative promoter) in the two *V. inaequalis* strains S755 and Rs552. **A**, Relative *Cyp51A* expression in S755 and Rs552 in presence or absence of tebuconazole or fengycin. The presence of different letters in each molecule indicates a significant difference among the two strains according to the ANOVA-Tukey test at α=0.05. **B**, Simplified scheme of the *Cyp51A* upstream region alignment. Grey, conserved sequence; yellow, 499 bp insertion cut in two segments by 613 bp insertion; blue, 613 bp insertion; green, deleted sequence; orange, single nucleotide polymorphism. 3a-27–10 corresponds to a sensitive reference strain from Villani et al. (2016). **C**, DNA-binding motif for transcription factors from MEME Suite (Bailey and Elkan, 1994). **D**, Position of DNA-binding motifs in the *Cyp51A* upstream region of S755 and Rs552. **E**, DNA-binding motifs obtained by MEME suite. **F**, DNA-binding motif positioning obtained by MEME suite in S755 and Rs552.

review was used to select five motifs to identify DNA-binding transcription factors (Fig. 4E). Of the five motifs found, only two were found to correspond to both the Rs552 and S755 strains: ATCNNNNAT and CGG-Nx-CCG (Fig. 4F). The ATCNNNNAT motif was found twice in strain S755 and four times in the region upstream of the *Cyp51A* gene. In Rs552, one motif was repeated twice (ATCGGTTCAT), in the 613 bp insertion repeat. The other two motifs (ATCCCAAGAT and ATCCCTGAAT) were found in both strains. The CGG-Nx-CCG motif was found once in S755 and three times in Rs552. The motif common to both strains is CGG-N16(6)-CCG. The second motif in Rs552 was also repeated, as it was also found in the 613 bp CGG-N11(5)-CCG insertion. The motifs found may explain the increased expression of *Cyp51A* in Rs552, as this strain would have more DNA binding sites than S755.

3.6. Rs552 has increased membrane efflux pump activity compared to S755

The potential involvement of efflux pumps as a mechanism of reduced sensitivity to azoles and fengycin was examined phenotypically and genetically in both strains of *V. inaequalis*. Tolnaftate is an antifungal agent used to treat dermatophytic fungi and is also an indicator of multidrug resistance (MDR) in plant pathogenic fungi overexpressing efflux pumps (Leroux and Walker, 2010; Omrane et al., 2015). Interestingly, tolnaftate significantly inhibited the growth of the sensitive strain S755 at different concentrations (IC_{50} value of 0.66 mg/L), whereas no inhibitory activity was observed on the strain Rs552 (*data not shown*). These results indicate a potential involvement of efflux pumps in the reduced sensitivity of Rs552 to tebuconazole.

Efflux pump modulators (EPMs) were tested with tebuconazole, fengycin and tolnaftate to determine whether these pumps contribute to the mechanisms involved in the reduced sensitivity of Rs552. Firstly, the interaction of EPMs with tebuconazole was evaluated. At concentrations close to the IC_{50} value of each strain, synergy was observed with amitriptyline and chlorpromazine, but not with verapamil (Fig. 5 Aa). Chlorpromazine was synergistic with tebuconazole at both concentrations tested, 4.5 and 7 mg/L, whereas amitriptyline was only slightly synergistic at 7 mg/L. At 7 mg/L, the interaction ratios (IRs) for chlorpromazine appeared higher than for amitriptyline, with IRs between 1.6 and 2.9 for amitriptyline and between 2.6 and 7.7 for chlorpromazine. In addition, higher IRs were also calculated with chlorpromazine at 7 mg/L for Rs552 (2.7–7.7) compared with S755 (2.6–4.8). For the other concentrations, the interactions between EPMs and tebuconazole were only additive (Table S3a). Between 0.8 and 1.7 mg/L tebuconazole, S755 was completely inhibited, whereas no inhibition was observed for Rs552 at concentrations between 0.008 and 0.17 mg/L (*data not shown*). In contrast to the synergies obtained with tebuconazole, no synergistic interaction occurred between fengycin and the EPMs tested at concentrations close to the IC_{50} for S755 or higher for Rs552 (Fig. 5Ab). The interactions were mostly additive and even slightly antagonistic, even at the other concentrations tested (Table S3b). EPMs were also combined with tolnaftate. Synergy was mainly observed with chlorpromazine, particularly on Rs552, with a high IR of 10 calculated between chlorpromazine at 7 mg/L and tolnaftate at 5 mg/L (Fig. 5 Ac). Synergy was also observed for S755 with amitriptyline 7 mg/L. The combination of verapamil and tolnaftate was not synergistic on both strains. The RI of tolnaftate was mainly additive at other concentrations (Table S3c). On the basis of these results, efflux pumps appear to be involved in the reduced sensitivity of Rs552 to azoles.

From the whole genome sequences of both strains, four *ABC* pump genes and one *MFS* pump gene were found (Fig. 5B). For the *MFS* pump gene, a single silent mutation was found in Rs552. However, for the *ABC* pump genes, an increased number of silent and non-silent mutations were detected in Rs552 (Fig. 5B, Table S4). Non-silent mutations can influence the protein through amino acid changes such as in the ABC1 (I1229M, V1299I), ABC2 (D752N, K846R, V929I, S971P, N1436S), ABC3 (A977S, S1051N) and ABC4 (A757T, S816 A) proteins. The I1229M substitution in the *ABC1* pump can modify the structure of the protein, as methionine is a sulphur amino acid that can form disulfide bridges.

In addition, variations in the respective putative promoter regions of the five efflux pump genes detected were analysed. No polymorphisms were observed for the *MFS* and *ABC2* genes. However, the putative promoter regions of the *ABC1* and *ABC4* genes showed several polymorphisms (Table S4) which could affect gene expression. In addition, the CGG-Nx-CCG binding motif, found in *ABC* pumps, was detected in the *ABC1* and *ABC4* genes. The CGG-Nx-CCG motif was found three times in the promoter regions of both pumps in both strains. For *ABC1*, the CGG-N15-CCG, CGG-N18-CCG, CGG-N22(18)-CCG motif was located at 675 th, 641st, and 428 th 5′ bases in Rs552 and at 699 th, 665 th and 435 th 5′ bases in S755. For *ABC4*, the CGG-N19-CCG, CGG-N13-CCG and CGG-N18-CCG motifs were located at 486 th, 364 th and 313 th 5′ bases in S755, and at 489 th, 367 th and 316 th 5′ bases in Rs552. These

(A)

			Efflux pump modulator					
(a)			Amitriptyline		Chlorpromazine		Verapamil	
	Strain	Concentration (mg/L)	4.5	7	4.5	7	4.5	7
Tebuconazole	S755	0.008	1.1	**1.6**	**2.5**	**2.6**	1.1	1.0
		0.012	0.9	**2.5**	**2.9**	**3.1**	1.2	0.9
		0.017	1.4	**2.9**	**4.0**	**4.8**	1.1	1.0
	Rs552	0.8	1.1	**1.6**	**4.1**	**7.7**	0.9	0.8
		1.2	1.1	**1.6**	**4.5**	**6.5**	0.9	0.7
		1.7	1.2	**1.6**	**3.6**	**2.7**	0.9	0.8
(b)			Amitriptyline		Chlorpromazine		Verapamil	
	Strain	Concentration (mg/L)	4.5	7	4.5	7	4.5	7
Fengycin	S755	0.01	0.9	0.9	0.9	0.7	0.9	1.0
		0.02	0.9	0.8	0.8	0.6	0.9	1.0
		0.04	0.6	0.6	0.5	0.3	0.6	0.8
	Rs552	1	0.8	0.8	0.8	0.7	0.9	1.0
		2	0.6	0.6	0.7	0.7	0.8	1.0
		4	0.8	0.6	0.6	0.5	0.9	0.9
(c)			Amitriptyline		Chlorpromazine		Verapamil	
	Strain	Concentration (mg/L)	4.5	7	4.5	7	4.5	7
Tolnaftate	S755	0.125	1.0	1.0	1.1	1.2	1.0	1.0
		0.25	1.0	1.1	1.1	**1.7**	1.3	1.2
		0.5	1.1	**1.7**	**1.7**	**3.3**	1.1	1.0
	Rs552	1.25	0.8	0.8	**1.5**	**2.8**	0.8	0.9
		2.5	0.9	0.9	**1.9**	**2.8**	0.9	1.0
		5	0.9	1.0	**3.1**	**10.1**	0.9	0.9

(B)

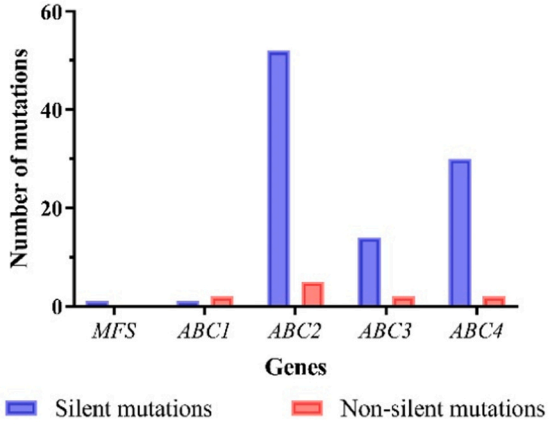

Fig. 5. Biochemical and genetic analysis of efflux pumps in the two *V. inaequalis* strains S755 and Rs552. **A**, Interaction ratios (IRs) between efflux pump modulators (amitriptyline, chlorpromazine, verapamil) and tebuconazole (a), fengycin (b), and tolnaftate (c). The used concentrations of fungicides are close to the IC_{50} value obtained for each strain. Synergy is indicated by bold IR values. **B**, Number of silent and non-silent mutations found in the ABC- and MFS-encoding genes in S755 and Rs552.

motifs located in the upstream regions would influence the level of expression of the genes encoding the targeted efflux pumps, which could explain the difference observed between the two strains in terms of their efflux pump activity.

3.7. Rs552 and S755 vary slightly in sterol and phospholipid composition

Sterols in the mycelium of the two strains of *V. inaequalis* were analysed and quantified by GC-MS/FID. Several sterols were identified, mainly ergosta-5,8-dien-3-ol, ergosta-7,22-dien-3-ol and ergosta-5,24-dien-3-ol in a lower percentage (Fig. 6A, Table S5). These sterols are derivatives of ergosterol. Squalene, a sterol precursor in the sterol biosynthesis pathway, was also identified. Quantification of total sterols revealed that there was no quantitative difference between the two strains (6.20 ± 1.79 and 6.27 ± 1.66 µg sterols/mg dry weight for S755 and Rs552 respectively, *data not shown*), indicating that the strains produce the same total amount of total sterols. Qualitative analysis showed no significant difference between the different sterols, with the exception of ergosta-7,22-dien-3-ol, which was detected in a higher proportion in strain Rs552 (21 % ± 0.32) compared with strain S755 (16.3 % ± 1.25) (Fig. 6A, Table S5).

Phospholipid analysis was used to identify the different classes of phospholipids and their associated fatty acid chains in the two fungal strains. The relative composition of the phospholipid classes showed that both strains are composed of phosphatidylinositol (PI), phosphatidylethanolamine (PE), phosphatidylcholine (PC), lysophosphatidylcholine (LPC), phosphatidylserine (PS), lysophosphatidylethanolamine (LPE) and traces of phosphatidylglycerol (PG) (Fig. 6B). PI followed by PE and PC represented 46 % ± 4.44, 33 % ± 3.09 and 13 % ± 2.3 respectively for strain S755, and 46.7 % ± 5.68, 33 % ± 4.5 and 12 % ± 2.28 for strain Rs552 (Table S5). There were no significant differences between the two strains for each phospholipid class (Fig. 6B). Quantification of total phospholipids revealed that there was no quantitative difference between the two strains (97.14 ± 7.84 and 102.64 ± 24.87 µg phospholipids/mg dry weight for S755 and Rs552 respectively, *data not shown*), indicating that the strains produced the same total amount of total phospholipids.

Within each phospholipid class, the fatty acids were determined and analysed. Significant differences were obtained for the PI, LPC and LPE classes (Fig. 6C, D, E) while no difference was observed for the PE, PC, PS and PG classes (Fig. S4). The main change was in PI(C16:0/C18:1), which was lower in proportion in Rs552 than in S755 (Fig. 6C, Table S5). For LPC, the minor forms LPC(16:0) and LPC(18:0) were present in a higher proportion in Rs552 than in S755 (Fig. 6D). And for LPE, the major form LPE(18:1) was in lower proportion in Rs552 than in S755 while the minor form LPE(16:0) was in higher proportion (Fig. 6E).

Differences in the sterol and phospholipid compositions of the two strains were observed. Although these differences do not appear to be very significant, they could be linked to different membrane lipid compositions and a particular cellular function between the two strains.

4. Discussion

4.1. Antifungal activity against V. inaequalis varies according to lipopeptide family

Antifungal activity tests revealed variable activity profiles for the three lipopeptide families against the two *V. inaequalis* strains used, S755 and Rs552. The bioactivity of lipopeptides has been well studied against a wide range of phytopathogens, such as *Botrytis cinerea*, *Sclerotinia sclerotiorum* (Botcazon et al., 2022) and *Pyricularia grisea* (Zhang and Sun, 2018) for fengycin; *Zymoseptoria tritici* (Mejri et al., 2018) for mycosubtilin, and *Phytophthora capsici*, *Fusarium graminearum* and *Rhizoctonia solani* for iturin A (Liu et al., 2007). However, the antifungal activity of lichenysin and pumilacidin is poorly documented. Interestingly, we have revealed here that lichenysin and pumilacidin (belonging to the surfactin family) do not have antifungal activity against *V. inaequalis* as previously shown for surfactin (Desmyttere et al., 2019) compared to mycosubtilin and iturin A (belonging to the iturin family). This family lipopeptide-dependent bioactivity is probably due to variations in the structure of the peptide part, which are stronger at the inter- than at the intra-family level (Fig. 1B). Within the same family, variations in the fatty acid chain can also modulate biological activity, as it was demonstrated with the activity of mycosubtilin against *Botrytis cinerea* (the longer the fatty acid chain, the better the activity) (Bechet et al., 2013). This was confirmed in this work with the activity of

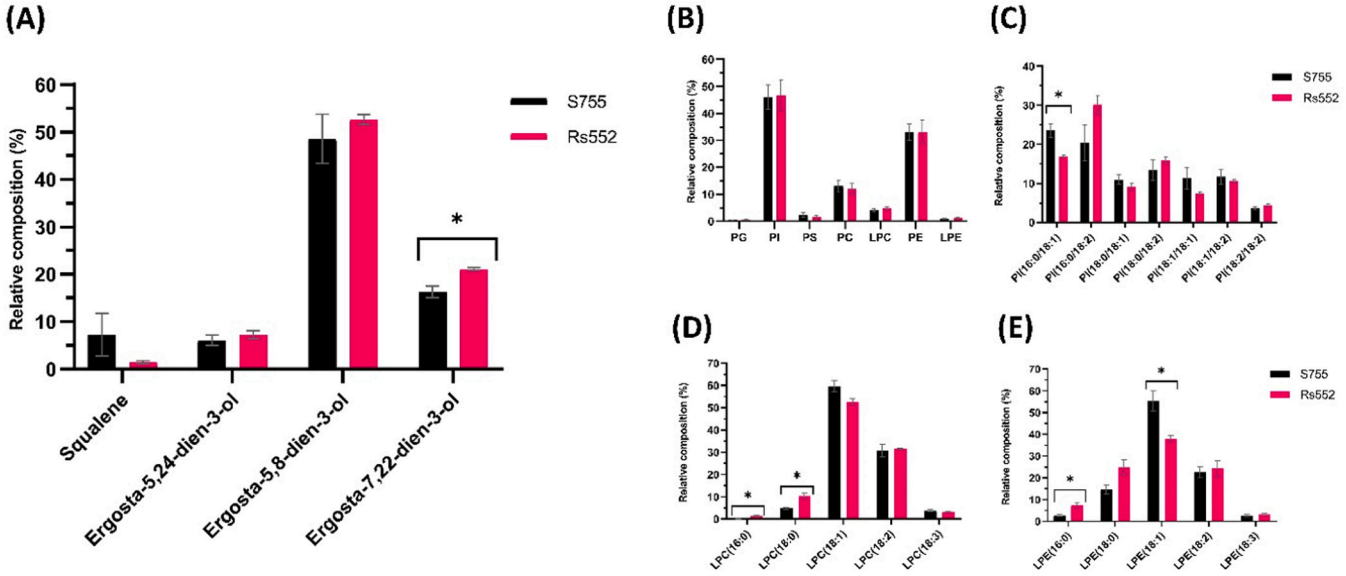

Fig. 6. Comparison of the relative composition of both total sterols and total phospholipids in the two *V. inaequalis* strains S755 and Rs552. **A**, Relative composition comparison of total sterol derivatives. **B**, Relative composition comparison of different classes of phospholipids: phosphatidylglycerol (PG), phosphatidylinositol (PI), phosphatidylserine (PS), phosphatidylcholine (PC), lysophosphatidylcholine (LPC), phosphatidylethanolamine (PE), and lysophosphatidylethanolamine (LPE); **C**, Comparison of the relative composition of PI; **D**, Relative composition comparison of LPC; **E**, Comparison of the relative composition of LPE. The presence of an asterisk indicates a significant difference among the two strains according to the ANOVA-Tukey test at α=0.007.

mycosubtilin (with 16 and 17 carbon fatty acid chains predominating) being significantly higher against both strains of *V. inaequalis* compared to Iturin A (which is predominantly produced with C14 and C15 fatty acid chains).

Interestingly, fengycin exhibited the highest antifungal activity against S755 of all the lipopeptides evaluated, with a level similar to that conferred by the pure active substance, tebuconazole, but lower than that of tetraconazole. The IC_{50} measured is one of the lowest cited in the literature for fengycin. This level of activity could be due to a stronger interaction of this molecule with the components of the plasma membrane of sensitive strain S755. For the binary mixtures, all the mixtures with fengycin showed similar levels of activity on S755 to those of fengycin alone, suggesting that there is no enhancement of its activity by the other lipopeptides. As highlighted previously, fengycin showed no antifungal activity on Rs552 when tested alone (Desmyttere et al., 2019), whereas fengycin-lichenysin and fengycin-pumilacidin mixtures showed a significant effect on this strain (Fig. 1A). Such 'mixture-induced' biological activity has already been demonstrated for the fengycin-surfactin mixture, suggesting a similar role for different members of the surfactin family in this effect. This could be due to a chemical interaction or to the formation of mixed micelles between the combined lipopeptides, which could result in a modification of their properties. Synergistic effects between other lipopeptide combinations have already been reported in several fungi (Maget-Dana et al., 1992; Ongena et al., 2007; Romero et al., 2007; Desmyttere et al., 2019).

4.2. Increased expression of Cyp51A and overactivity of the membrane efflux pump are probably the main mechanisms responsible for the reduced sensitivity to azoles in Rs552

Reduced sensitivity to azoles can be explained by three different mechanisms, including mutations in the *Cyp51A* gene, increased expression of this gene and/or increased activity of membrane efflux pumps. Surprisingly, we detected a S183C substitution in the *Cyp51A* gene of strain S755, while no change was found in the reduced-susceptibility strain Rs552. Other substitutions are known to reduce azole sensitivity in resistant strains of *V. inaequalis*, including Y133F (Yaegashi et al., 2020) and M141T (Hoffmeister et al., 2021). Nevertheless, the substitution found in S755 has never been reported. However, no structural modifications or changes in the opening of the catalytic pocket were detected, suggesting that the S183C substitution found in S755 would have no impact on sensitivity to azole fungicides. Quantification of expression showed that, unlike 755, Rs552 constitutively overexpressed the *Cyp51A* gene (Fig. 4A). Furthermore, *Cyp51A* expression was not induced by treatment with tebuconazole and fengycin in either strain. In previous work, resistance of *V. inaequalis* to difenoconazole and/or myclobutanil was associated with an increased expression of the *Cyp51A* gene (Schnabel and Jones, 2001; Villani et al., 2016). Therefore, it is clearly established that the observed constitutive increased expression of *Cyp51A* may contribute to the reduced sensitivity to azoles in Rs552.

To better understand the increased expression of *Cyp51A* in strain Rs552 at the molecular level, a comparison of the putative promoter upstream of the *Cyp51A* gene in different strains with different sensitivities to tebuconazole was undertaken. A 499 bp insertion in both strains and two 613 bp insertions in strain Rs552 were identified in the *Cyp51A* promoter region. The 499 bp insertion has previously been observed in *V. inaequalis* strains susceptible and resistant to myclobutanil/difenoconazole, and therefore does not always appear to correlate with the resistance mechanism (Schnabel and Jones, 2001; Villani et al., 2016). However, Schnabel and Jones (2001) identified a 553 bp insertion in the promoter region of several resistant strains. This sequence, inserted at the same position of the 613 bp insertion, could act as a transcriptional enhancer of *Cyp51A* and was correlated with myclobutanil resistance in the Ent2 strain (ACC#AF227917). This 613 bp insertion in Rs552 could therefore contribute to the *Cyp51A* increased expression. These two reports conclude that these insertions may explain resistance in some strains, but not in all, suggesting the existence of another resistance mechanism.

In addition to this insertion analysis, a bioinformatic analysis of *Cyp51A* transcription factor binding sites was carried out. Transcription factors are protein-based molecules that play a crucial role in the regulation of gene expression. They are formed by at least two core structural domains: (i) an effector domain acting as a regulating part able to detect signals mediated by intracellular metabolites or by signals originating from the extracellular environment (leading to repression or activation of gene expression) and (ii) a DNA binding domain (usually including helix-turn-helix, helix-loop-helix, zinc finger or leucine zipper motifs) that specifically recognizes and binds to regulatory sequences (transcription factors binding sites) located in promoter regions of target genes (He et al., 2023). Since transcription factors can control gene expression, an identification of the corresponding binding sites would provide a valuable knowledge. Two putative motifs have already been identified in *A. fumigatus*, corresponding to possible DNA-binding sites for the SrbA and AtrR transcription factors. The SrbA protein is a basic helix-loop-helix transcription factor belonging to the sterol regulatory element binding protein family (Linde et al., 2012; Chung et al., 2014), while the AtrR protein is a fungal specific Zn2-Cys6 transcription factor (Hagiwara et al., 2017). It has been reported that these two activator-like proteins play a key role in the regulation of *Cyp51A* gene expression by binding to two conserved sequences in the promoter region (Blosser and Cramer, 2012; Chung et al., 2014; Hagiwara et al., 2017; Todd et al., 2006 Willger et al., 2008). For instance, functional analyses using mutagenesis revealed that AtrR plays a crucial role in resistance to azole fungicides in *A. fumigatus*, *A. oryzae*, and *A. nidulans* through the regulation of genes involved in ergosterol biosynthesis (Hagiwara et al., 2017). Likewise, a mutagenesis approach demonstrated the importance of SrbA in the resistance of *A. fumigatus* to the azole fungicides, including fluconazole and voriconazole (Willger et al., 2008). Furthermore, chromatin immunoprecipitation followed by massively parallel DNA sequencing (ChIP-seq) assays confirmed the role of SrbA in the resistance to azoles and the regulation of ergosterol biosynthesis and revealed new roles for SrbA, including nitrate assimilation and heme biosynthesis (Chung et al., 2014). Interestingly, both transcription factors SrbA and AtrR are present in S755 and Rs552, thus explaining at least the low basal *Cyp51A* expression recorded in S755. Nevertheless, we detected more transcription factor binding sites in Rs552 (seven DNA binding sites) than in S755 (three DNA binding sites), which could correlate with the increased expression of *Cyp51A* scored in Rs552. Indeed, it is likely that an occurrence of increased copies of transcription factor biding sites would enhance the rate of gene expression, by probably allowing more bindings events between the transcription factors and the corresponding binding sites (Das et al., 2017). However, to determine the role of these binding sites in Rs552 and S755 and their associated transcription factors, further functional assays would be required.

The last hypothesis concerns efflux pumps in *V. inaequalis,* whose multiple resistance to fungicides has not been directly linked to efflux pumps (Chatzidimopoulos et al., 2022). Tolnaftate, a pump substrate of ABC transporters and MFS pumps, has previously been used for the MDR phenotype on other plant pathogenic fungi (Omrane et al., 2015). High levels of tolnaftate resistance (>25 and >100) between wild-type and resistant strains of *B. cinerea* have only been calculated for MDR strains with efflux pumps involved in the resistance mechanism (Kretschmer et al., 2009; Leroux and Walker, 2013). Thus, as tolnaftate showed no antifungal activity on Rs552, efflux pumps may contribute to the reduced sensitivity of this strain to azoles and probably to other fungicides.

Several EPMs have already shown synergy with azoles, particularly in strains overexpressing ABC transporters (Hayashi et al., 2002a). Amitriptyline and chlorpromazine have been identified as modulators of ABC transporters, but also verapamil, which potentially blocks both ABC

and MFS pumps (Hayashi et al., 2003; Leroux and Walker, 2013). The addition of amitriptyline and chlorpromazine appears to enhance the activity of tebuconazole in sensitive and reduced sensitivity strains. These results indicate the presence of at least one efflux pump capable of facilitating tebuconazole efflux. IRs were higher with chlorpromazine than with amitriptyline, indicating that amitriptyline may have less binding affinity with the transporter than chlorpromazine at the concentrations tested. Hayashi et al. (2003) showed that the more resistant *B. cinerea* strains were to oxpoconazole, the greater their synergy with chlorpromazine. Thus, the higher IRs on Rs552 with chlorpromazine may indicate an increase in efflux for this strain. Chlorpromazine has previously shown synergistic activity with tebuconazole on sensitive and resistant strains of *B. cinerea,* and IR values appear to be linked to the level of expression of *BcatrD* (gene encoding an ABC transporter) (Leroux and Walker, 2013). Furthermore, synergy with tolnaftate was also observed with chlorpromazine, with a high IR on Rs552, which was only noticed on MDR strains of *Z. tritici* strains (Leroux and Walker, 2010). In contrast to chlorpromazine, the combination of verapamil with tebuconazole and tolnaftate resulted in additive interactions. As suggested by Hayashi et al. (2003), ABC transporters may have one or more specific receptors for modulators and, therefore, verapamil may have less affinity for these receptors than chlorpromazine at these concentrations.

The higher IR in the Rs552 strain suggests that efflux is more important in this strain. At least two transporters are involved in azole efflux in *B. cinerea*, including the ABC transporter *BcatrD* and the MFS pump, Bcmfs1 (Hayashi et al., 2002a, 2002b; Leroux and Walker, 2013). To this purpose, an analysis was carried out to identify the genes encoding the ABC transporter and the MFS pump from the two genomic sequences of the two *V. inaequalis* strains. No polymorphisms were found in the *MFS1* gene or in the promoter region. However, several mutations were found in the genes encoding the ABC pump. It is not easy to say whether these mutations have an impact or not on the protein. Analysis of the promoter regions of the *ABC1* and *ABC4* genes revealed the presence of the *AtrR* transcription factor binding motif. For both genes, this motif was found three times in both strains. Consequently, this motif would not necessarily be involved in the greater efflux of tebuconazole in Rs552. However, insertions of 8 and 17 bases in the upstream region of *ABC1* in S755 may displace *AtrR* binding sites, potentially limiting gene expression.

4.3. Lipid composition and vesicle formation may play a role in the reduced sensitivity of Rs552 to fengycin

As lipopeptides interact with membrane lipids, a comparison of lipid composition between the two strains of *V. inaequalis* was performed to better understand fungal variability in sensitivity to fengycin. No quantitative distinction was recorded between the two strains with regard to total sterols and phospholipids as a whole. Nevertheless, some differences were observed in lipid analysis, particularly in ergosta-7,22-dien-3-ol, PI(16:0/18:1), LPC(C16:0), LPC(C18:0), LPE(16:0), and LPE (C18:1). These differences may be associated with the variability in sensitivity obtained between S755 and Rs552.

The fungal plasma membrane is made up of a lipid bilayer mainly composed of phospholipids (Weete, 2012). Ergosterol, the second major component, regulates the fluidity and permeability of the membrane (Deacon, 2006; Pan et al., 2018; Stephenson, 2010). Although Vijaya Palani and Lalithakumari (1999) found no disparity in ergosterol levels between penconazole-sensitive and -resistant strains; Shirane et al. (1996) found differences in ergosterol derivatives between fenarimol-sensitive and -resistant strains of *V. inaequalis*, with the resistant strain containing more ergosterol than the sensitive strain. However, it is not clear whether ergosterol affects the mode of action of fengycin, with some reports suggesting a lesser antagonistic effect of ergosterol than cholesterol on fengycin activity. Interesting, Vanittanakom et al. (1986) demonstrated the formation of complexes between fengycin and ergosterol. Other studies have shown that the activity of fengycin is negatively correlated with the ergosterol content; as the amount of ergosterol increases (*in vitro* experiments or on artificial membrane models), the bioactivity of fengycin decreases. (Botcazon et al., 2022; Mantil et al., 2019b; Wise et al., 2014). These findings are consistent with our results showing significantly higher proportions of ergosta-7,22-dien-3-ol in Rs552 compared to S755. The higher level of this compound may contribute to the reduced sensitivity of Rs552 to fengycin. However, iturinic compounds are also capable of interacting with ergosterol in an *in vitro* membrane simulation system (Maget-Dana and Peypoux, 1994; Nasir and Besson, 2012). If the membrane proportions of ergosterol are different in our biological membranes, we would therefore expect variations in sensitivity to iturin or mycosubtilin between the two strains of *V. inaequalis,* which is not the case.

Phospholipids also play an essential role in membrane composition and interaction with fengycin. Rs552 and S755 contain mainly PI, PE and PC, which differs from the well-known composition of the yeast plasma membrane, where the majority of phospholipids are PS, followed by PI, PE and PC (Van Meer et al., 2008). PI and its derivatives, phosphoinositides, are key mediators in signal transduction (El-Bacha and Torres, 2016). They can also dynamically recruit soluble and membrane proteins by phosphorylation and dephosphorylation (Harayama and Riezman, 2018). Lysophospholipids are also messenger lipids. They can easily leave the membrane, as they only have a single fatty acid (Tan et al., 2020). The presence of short, unsaturated fatty acids in phospholipids increases membrane fluidity, which increases membrane sensitivity to fengycin (Vanittanakom et al., 1986; Wise et al., 2014). In S755, there is more PI(C16:0/C18:1) than in Rs552 (Fig. 6C), which could explain the greater sensitivity of this strain to fengycin, disrupting the membrane and leading to cell death. Negatively charged lipids (PG, PI and PS), short-chain unsaturated fatty acids (phospholipids) and a low concentration of ergosterol (Mantil et al., 2019c; Wise et al., 2014; Zakharova et al., 2019), have also been shown to play a key role in membrane fluidity, promoting the interaction between fengycin and fungal plasma membranes. In the activity of fengycin, the role of phospholipids has nevertheless been mentioned as secondary to that of ergosterol (Mantil et al., 2019a). These results were mainly observed using a cell membrane simulation system *in vitro,* and it is not yet clear whether this can be transposed *in vivo*.

Fengycin induced morphological and cytological changes with the formation of vesicles in the mycelium of both strains, but with a lower occurrence in Rs552. These vesicles resemble a swelling of the cell until it bursts. Morphological changes in fungal mycelium after treatment with fengycin have already been described in the literature. Vanittanakom et al. (1986) demonstrated the existence of bulging in certain fungi. Zhang and Sun (2018) and Xue et al.(2023) showed the formation of vesicles in *P. grisea* and *F. oxysporum* that were about to burst or had burst at the hyphal level. Vesicles were also observed in *B. cinerea* in the presence of fengycin (Botcazon et al., 2022). The same spherical vesicle shapes were observed in *S. Sclerotiorum* (Yang et al., 2020) and *Alternaria solani* (Mu et al., 2023) in contact with filtrates of *B. amyloliquefaciens* containing fengycin. The formation of such a structure may be due to the mode of action of fengycin targeting plasma membranes, ultimately leading to cell leakage and membrane rupture, as well as cell wall synthesis. In its interaction with the membrane, it is likely that fengycin directly or indirectly influences the synthesis of wall components. As the cell wall of *V. inaequalis* is composed of glucans, mannans and chitin (Rocafort et al., 2023), it is possible that fengycin disrupts membrane enzymes such as glucan synthase and chitin synthase, for example, which may be involved in vesicle generation.

5. Conclusion

Our findings suggest that the reduced sensitivity of Rs552 to azole fungicides is likely mainly due to a constitutive increased expression of *Cyp51A* coupled with an increased efflux by membrane pumps.

Increased *Cyp51A* expression may or may not lead to increased ergosterol levels in the fungal plasma membrane. Hence, the similar sensitivity of both strains highlighted to the iturin family lipopeptides iturin A and mycosubtilin suggests that the rates of ergosterol in the membrane are not altered in both strains, despite increased proportions of total ergosta-7,22-dien-3-ol were recorded in Rs552. By contract, the reduced sensitivity to fengycin in Rs552 was correlated with low vesicle formation in fungal hyphae, which could result from changes in membrane phospholipid composition. Although the overactivity of the membrane efflux pump is probably involved in the reduced sensitivity to azoles, the involvement of this mechanism in the reduced sensitivity to fengycin was not clearly demonstrated since it depends on whether the biomolecule enters the fungal cells. Curiously, in the presence of EPM, fengycin did not exhibit any synergism, suggesting that entry of fengycin into fungal cells is unlikely. Hence, the reduced sensitivity to fengycin in Rs552 does not appear to be attributable to a mechanism of cellular uptake and efflux. Nevertheless, a high preponderance of efflux pumps in the fungal plasma membrane could affect the interaction of fengycin with membrane lipids *via* an indirect physical effect such as competition.

Funding

This work was supported by the Hauts-de-France Regional Council (France), the CPER BiHauts Eco de France (France), with co-funding from Junia (France), the University of Liège (Belgium) (project PHENIX biocontrol, FEDER program 2021-2027) and the F.R.S-FNRS (Belgium) (PDR Project Surfasymm, grant T.0063.19).

CRediT authorship contribution statement

Alexis Hoste: Investigation. **Valentin Fiévet:** Formal analysis. **Karin Sahmer:** Software, Methodology, Formal analysis. **Philippe Compère:** Methodology, Formal analysis. **Justine Jacquin:** Writing – original draft, Methodology, Investigation, Formal analysis, Conceptualization. **Ali Siah:** Writing – original draft, Visualization, Methodology, Formal analysis. **Aline Leconte:** Writing – original draft, Visualization, Methodology, Investigation, Formal analysis, Conceptualization. **Philippe Jacques:** Writing – review & editing, Writing – original draft, Validation, Supervision, Project administration, Funding acquisition, Conceptualization. **Matthieu Duban:** Resources, Investigation, Formal analysis. **Anissa Lounès-Hadj Sahraoui:** Methodology, Formal analysis. **Amaury Farce:** Visualization, Methodology, Formal analysis. **Jérôme MUCHEMBLED:** Writing – review & editing, Writing – original draft, Validation, Supervision, Project administration, Methodology, Funding acquisition, Formal analysis, Data curation, Conceptualization. **Frédéric Laruelle:** Methodology, Investigation, Formal analysis. **Magali Deleu:** Writing – review & editing, Writing – original draft, Validation, Supervision, Project administration, Funding acquisition, Formal analysis, Conceptualization. **Pauline Trapet:** Methodology, Formal analysis. **François Coutte:** Writing – review & editing, Writing – original draft, Validation, Supervision, Project administration, Methodology, Funding acquisition, Formal analysis, Data curation, Conceptualization. **Caroline Deweer:** Resources, Formal analysis.

Declaration of Completing Interest

Most of the authors declare no conflicts of interest. François Coutte. and Philippe Jacques are co-founders of Lipofabrik company (Elephant Vert group).

Data availability

Data will be made available on request.

Appendix A. Supporting information

Supplementary data associated with this article can be found in the online version at doi:10.1016/j.micres.2024.127816.

References

Aranda, F.J., Teruel, J.A., Ortiz, A., 2005. Further aspects on the hemolytic activity of the antibiotic lipopeptide iturin A. Biochim. Biophys. Acta Biomembr. 1713, 51–56. https://doi.org/10.1016/j.bbamem.2005.05.003.

Aranda, F.J., Teruel, J.A., Ortiz, A., 2023. Recent advances on the interaction of glycolipid and lipopeptide biosurfactants with model and biological membranes. Curr. Opin. Colloid Interface Sci. 68, 101748 https://doi.org/10.1016/j.cocis.2023.101748.

Bailey, T.L., Elkan, C., 1994. Fitting a mixture model by expectation maximization to discover motifs in biopolymers. Proc. Int. Conf. Intell. Syst. Mol. Biol. 2, 28-36. PMID: 7584402.

Bechet, M., Guy-Castera, J., Guez, J.S., Chihib, N., Coucheney, F., Coutte, F., Fickers, P., Leclere, V., Wathelet, B., Jacques, P., 2013. Production of a novel mixture of mycosubtilins by mutant of Bacillus subtilis mutants. Bioresour. Technol. 145, 264–270. https://doi.org/10.1016/j.biortech.2013.03.123.

Bedart, C., Renault, N., Chavatte, P., Porcherie, A., Lachgar, A., Capron, M., Farce, A., 2022. SINAPs: a software tool for analysis and visualization of interaction networks of molecular dynamics simulations. J. Chem. Inf. Model. 62, 1425–1436. https://doi.org/10.1021/acs.jcim.1c00854.

Blosser, S.J., Cramer, R.A., 2012. SREBP-dependent triazole susceptibility in aspergillus fumigatus is mediated through direct transcriptional regulation of erg11A (cyp51A). Antimicrob. Agents Chemother. 56, 248–257. https://doi.org/10.1128/aac.05027-11.

Botcazon, C., Bergia, T., Lecouturier, D., Dupuis, C., Rochex, A., Acket, S., Nicot, P., Leclère, V., Sarazin, C., Rippa, S., 2022. Rhamnolipids and fengycins, very promising amphiphilic antifungal compounds from bacteria secretomes, act on Sclerotiniaceae fungi through different mechanisms. Front. Microbiol. 13, 977633 https://doi.org/10.3389/fmicb.2022.977633.

Bowen, J.K., Mesarich, C.H., Bus, V.G.M., Beresford, R.M., Plummer, K.M., Templeton, M.D., 2011. Venturia inaequalis: the causal agent of apple scab. Mol. Plant Pathol. 12, 105–122. https://doi.org/10.1111/j.1364-3703.2010.00656.x.

Buske, F.A., Bodén, M., Bauer, D.C., Bailey, T.L., 2010. Assigning roles to DNA regulatory motifs using comparative genomics. Bioinform 26, 860–866. https://doi.org/10.1093/bioinformatics/btq049.

Case, D.A., Ben-Shalom, I.Y., Brozell, S.R., Cerutti, D.S., Cheatham III, T.E., Cruzeiro, V. W.D., Darden, T.A., Duke, R.E., Ghoreishi, D., Giambasu, G., Giese, T., Gilson, M.K., Gohlke, H., Goetz, A.W., Greene, D., Harris, R., Homeyer, N., Huang, Y., Izadi, S., Kovalenko, A., Krasny, R., Kurtzman, T., Lee, T.S., LeGrand, S., Li, P., Lin, C., Liu, J., Luchko, T., Luo, R., Man, V., Mermelstein, D.J., Merz, K.M., Miao, Y., Monard, G., Nguyen, C., Nguyen, H., Onufriev, A., Pan, F., Qi, R., Roe, D.R., Roitberg, A., Sagui, C., Schott-Verdugo, S., Shen, J., Simmerling, C.L., Smith, J., Swails, J., Walker, R.C., Wang, J., Wei, H., Wilson, L., Wolf, R.M., Wu, X., Xiao, L., Xiong, Y., York, D.M., Kollman, P.A., 2019. AMBER 2019, University of California, San Francisco.

Cawoy, H., Mariutto, M., Henry, G., Fisher, C., Vasilyeva, N., Thonart, P., Dommes, J., Ongena, M., 2014. Plant defense stimulation by natural isolates of bacillus depends on efficient surfactin production. Mol. Plant Microbe Interact. 27, 87–100. https://doi.org/10.1094/MPMI-09-13-0262-R.

Chatzidimopoulos, M., Zambounis, A., Lioliopoulou, F., Vellios, E., 2022. Detection of Venturia inaequalis Isolates with Multiple Resistance in Greece. Microorganisms 10, 2354. https://doi.org/10.3390/microorganisms10122354.

Cheval, P., Siah, A., Bomble, M., Popper, A.D., Reignault, P., Halama, P., 2017. Evolution of QoI resistance of the wheat pathogen Zymoseptoria tritici in northern France. Crop Prot. 92, 131–133. https://doi.org/10.1016/j.cropro.2016.10.017.

Chowdhury, S.P., Uhl, J., Grosch, R., Alquéres, S., Pittroff, S., Dietel, K., Schmitt-Kopplin, P., Borriss, R., Hartmann, A., 2015. Cyclic lipopeptides of bacillus amyloliquefaciens subsp. plantarum colonizing the lettuce rhizosphere enhance plant defense responses toward the bottom rot pathogen rhizoctonia solani. Mol. Plant Microbe Interact. 28, 984–995. https://doi.org/10.1094/MPMI-03-15-0066-R.

Chung, D., Barker, B.M., Carey, C.C., Merriman, B., Werner, E.R., Lechner, B.E., Dhingra, S., Cheng, C., Xu, W., Blosser, S.J., Morohashi, K., Mazurie, A., Mitchell, T. K., Haas, H., Mitchell, A.P., Cramer, R.A., 2014. ChIP-seq and in vivo transcriptome analyses of the aspergillus fumigatus SREBP SrbA reveals a new regulator of the fungal hypoxia response and virulence. PLoS Pathog. 10, e1004487 https://doi.org/10.1371/journal.ppat.1004487.

Colby, S.R., 1967. Calculating synergistic and antagonistic responses of herbicide combinations. Weeds 15, 20–22. https://doi.org/10.2307/4041058.

Cools, H.J., Fraaije, B.A., 2013. Update on mechanisms of azole resistance in Mycosphaerella graminicola and implications for future control. Pest Manag. Sci. 69, 150–155. https://doi.org/10.1002/ps.3348.

Cordero-Limon, L., Shaw, M.W., Passey, T.A., Robinson, J.D., Xu, X., 2020. Cross-resistance between myclobutanil and tebuconazole and the genetic basis of tebuconazole resistance in Venturia inaequalis. Pest Manag. Sci. 77, 844–850. https://doi.org/10.1002/ps.6088.

Das, D., Dey, S., Brewster, R.C., Choubey, S., 2017. Effect of transcription factor resource sharing on gene expression noise. PLoS Comput. Biol. 13 (4), e1005491 https://doi.org/10.1371/journal.pcbi.1005491.

Deacon, J.W., 2006. Fungal biology, fourth edition, Blackwell Plublishing Ltd, Malden.

Deleu, M., Paquot, M., Nylander, T., 2005. Fengycin interaction with lipid monolayers at the air-aqueous interface-implications for the effect of fengycin on biological membranes. J. Colloid Interface Sci. 283, 358–365. https://doi.org/10.1016/j.jcis.2004.09.036.

Deleu, M., Paquot, M., Nylander, T., 2008. Effect of fengycin, a lipopeptide produced by Bacillus subtilis, on model biomembranes. Biophys. J. 94, 2667–2679. https://doi.org/10.1529/biophysj.107.114090.

Desmyttere, H., Deweer, C., Muchembled, J., Sahmer, K., Jacquin, J., Coutte, F., Jacques, P., 2019. Antifungal activities of Bacillus subtilis lipopeptides against two Venturia inaequalis strains with different sensitivity to tebuconazole. Front. Microbiol. 10, 2327. https://doi.org/10.3389/fmicb.2019.02327.

Dussert, E., Tourret, M., Dupuis, C., Noblecourt, A., Behra-Miellet, J., Flahaut, C., Ravallec, R., Coutte, F., 2022. Evaluation of Antiradical and Antioxidant Activities of Lipopeptides Produced by Bacillus subtilis Strains. Front. Microbiol. 13, 914713 https://doi.org/10.3389/fmicb.2022.914713.

El-Bacha, T., Torres, A.G., 2016. Phospholipids: Physiology, in: Caballero, B., Finglas, P. M., Toldrá, F. (Eds.), Encyclopedia of Food and Health. Academic Press, Oxford, pp. 352-359. https://doi.org/10.1016/B978-0-12-384947-2.00540-7.

Ermakova, E., Zuev, Y., 2017. Effect of ergosterol on the fungal membrane properties. All-atom and coarse-grained molecular dynamics study. Chem. Phys. Lipids 209, 45–53. https://doi.org/10.1016/j.chemphyslip.2017.11.006.

Falardeau, J., Wise, C., Novitsky, L., Avis, T.J., 2013. Ecological and mechanistic insights into the direct and indirect antimicrobial properties of bacillus subtilis lipopeptides on plant pathogens. J. Chem. Ecol. 39, 869–878. https://doi.org/10.1007/s10886-013-0319-7.

Hagiwara, D., Miura, D., Shimizu, K., Paul, S., Ohba, A., Gonoi, T., Watanabe, A., Kamei, K., Shintani, T., Moye-Rowley, W.S., Kawamoto, S., Gomi, K., 2017. A novel transcription factor Zn2-Cys6 AtrR plays a key role in an azole resistance mechanism of Aspergillus fumigatus by coregulating cyp51A and cdr1B expressions. PLoS Pathog. 13, e1006096 https://doi.org/10.1371/journal.ppat.1006096.

Hamamoto, H., Hasegawa, K., Nakaune, R., Lee, Y.J., Makizumi, Y., Akutsu, K., Hibi, T., 2000. Tandem repeat of a transcriptional enhancer upstream of the sterol 14α-demethylase gene (CYP51) in penicillium digitatum. Appl. Environ. Microbiol. 66, 3421–3426. https://doi.org/10.1128/aem.66.8.3421-3426.2000.

Harayama, T., Riezman, H., 2018. Understanding the diversity of membrane lipid composition. Nat. Rev. Mol. Cell Biol. 19, 281–296. https://doi.org/10.1038/nrm.2017.138.

Hayashi, K., Schoonbeek, H.-J., De Waard, M.A., 2002b. *Bcmfs1*, a novel major facilitator superfamily transporter from Botrytis cinerea, provides tolerance towards the natural toxic compounds camptothecin and cercosporin and towards fungicides. Appl. Environ. Microbiol. 68, 4996–5004. https://doi.org/10.1128/AEM.68.10.4996-5004.2002.

Hayashi, K., Schoonbeek, H., De Waard, M.A., 2003. Modulators of membrane drug transporters potentiate the activity of the DMI fungicide oxpoconazole against Botrytis cinerea. Pest. Manag. Sci. 59, 294–302. https://doi.org/10.1002/ps.637.

Hayashi, K., Schoonbeek, H., Waard, M., 2002a. Expression of the ABC transporter BcatrD from Botrytis cinerea reduces sensitivity to sterol demethylation inhibitor fungicides. Pestic. Biochem. Phys. 73, 110–121. https://doi.org/10.1016/S0048-3575(02)00015-9.

He, H., Yang, M., Li, S., Zhang, G., Ding, Z., Zhang, L., Shi, G., Li, Y., 2023. Mechanisms and biotechnological applications of transcription factors. Syn. Syst. Biotechnol. 8 (4), 565–577. https://doi.org/10.1016/j.synbio.2023.08.006.

Hoffmeister, M., Zito, R., Böhm, J., Stammler, G., 2021. Mutations in Cyp51 of Venturia inaequalis and their effects on DMI sensitivity. J. Plant Dis. Prot. 128, 1467–1478. https://doi.org/10.1007/s41348-021-00516-0.

Hulvey, J., Popko, J.T., Sang, H., Berg, A., Jung, G., 2012. Overexpression of ShCYP51B and ShatrD in sclerotinia homoeocarpa isolates exhibiting practical field resistance to a demethylation inhibitor fungicide. Appl. Environ. Microbiol. 78, 6674–6682. https://doi.org/10.1128/AEM.00417-12.

Jacques, P., 2011. Surfactin and Other Lipopeptides from Bacillus spp, in: Soberón-Chávez, G. (Ed.), Biosurfactants, Microbiology Monographs. Springer Berlin, Berlin, Heidelberg, pp. 57-91. https://doi.org/10.1007/978-3-642-14490-5_3.

Jones, G., Willett, P., Glen, R.C., 1995. Molecular recognition of receptor sites using a genetic algorithm with a description of desolvation. J. Mol. Biol. 245, 43–53. https://doi.org/10.1016/S0022-2836(95)80037-9.

Khajuria, Y.P., Akhoon, B.A., Kaul, S., Dhar, M.K., 2022. Secretomic insight into the pathophysiology of Venturia inaequalis: the Causative Agent of Scab, a Devastating Apple Tree Disease. Pathogens 12 (1), 66 https://doi: 10.3390/pathogens12010066.

Kretschmer, M., Leroch, M., Mosbach, A., Walker, A.-S., Fillinger, S., Mernke, D., Schoonbeek, H.-J., Pradier, J.-M., Leroux, P., De Waard, M.A., Hahn, M., 2009. Fungicide-Driven Evolution and Molecular Basis of Multidrug Resistance in Field Populations of the Grey Mould Fungus Botrytis cinerea. PLoS Pathog. 5, e1000696 https://doi.org/10.1371/journal.ppat.1000696.

Leconte, A., Tournant, L., Muchembled, J., Paucellier, J., Héquet, A., Deracinois, B., Deweer, C., Krier, F., Deleu, M., Oste, S., Jacques, P., Coutte, F., 2022. Assesment of lipopeptides mixtures produced by Bacillus subtilis as biocontrol products against apple scab (Venturia inaequalis). Microorganisms 10, 1810. https://doi.org/10.3390/microorganisms10091810.

Leroux, P., Walker, A.-S., 2010. Multiple mechanisms account for resistance to sterol 14α-demethylation inhibitors in field isolates of Mycosphaerella graminicola. Pest. Manag. Sci. 67, 44–59. https://doi.org/10.1002/ps.2028.

Leroux, P., Walker, A.-S., 2013. Activity of fungicides and modulators of membrane drug transporters in field strains of Botrytis cinerea displaying multidrug resistance. Eur. J. Plant Pathol. 135, 683–693. https://doi.org/10.1007/s10658-012-0105-3.

Lichtner, F.J., Jurick, W.M., Ayer, K.M., Gaskins, V.L., Villani, S.M., Cox, K.D., 2020. A genome resource for several north american venturia inaequalis isolates with multiple fungicide resistance phenotypes. Phytopathology 110, 544–546. https://doi.org/10.1094/PHYTO-06-19-0222-A.

Linde, J., Hortschansky, P., Fazius, E., Brakhage, A.A., Guthke, R., Haas, H., 2012. Regulatory interactions for iron homeostasis in Aspergillus fumigatus inferred by a Systems Biology approach. BMC Syst. Biol. 6, 6. https://doi.org/10.1186/1752-0509-6-6.

Liu, C.H., Chen, X., Liu, T.T., Lian, B., Gu, Y., Caer, V., Xue, Y.R., Wang, B.T., 2007. Study of the antifungal activity of Acinetobacter baumannii LCH001 in vitro and identification of its antifungal components. Appl. Microbiol. Biotechnol. 76, 459–466. https://doi.org/10.1007/s00253-007-1010-0.

Maget-Dana, R., Peypoux, F., 1994. Iturins, a special class of pore-forming lipopeptides: biological and physicochemical properties. Toxicology 87, 151–174. https://doi.org/10.1016/0300-483X(94)90159-7.

Maget-Dana, R., Thimon, L., Peypoux, F., Ptak, M., 1992. Surfactin/iturin A interactions may explain the synergistic effect of surfactin on the biological properties of iturin A. Biochimie 74, 1047–1051. https://doi.org/10.1016/0300-9084(92)90002-V.

Mantil, E., Buznytska, I., Daly, G., Lanoul, A., Avis, T.J., 2019a. Role of lipid composition in the interaction and activity of the antimicrobial compound Fengycin with complex membrane models. J. Membr. Biol. 252, 627–638. https://doi.org/10.1007/s00232-019-00100-6.

Mantil, E., Crippin, T., Avis, T.J., 2019b. Supported lipid bilayers using extracted microbial lipids: domain redistribution in the presence of fengycin. Colloids Surf. B: Biointerfaces 178, 94–102. https://doi.org/10.1016/j.colsurfb.2019.02.050.

Mantil, E., Crippin, T., Avis, T.J., 2019c. Domain redistribution within ergosterol-containing model membranes in the presence of the antimicrobial compound fengycin. Biochim. Biophys. Acta Biomembr. 1861, 738–747. https://doi.org/10.1016/j.bbamem.2019.01.003.

Marmorstein, R., Carey, M., Ptashne, M., Harrison, S.C., 1992. DNA recognition by GAL4: structure of a protein-DNA complex. Nature 356, 408–414. https://doi.org/10.1038/356408a0.

Mejri, S., Siah, A., Coutte, F., Magnin-Robert, M., Randoux, B., Tisserant, B., Krier, F., Jacques, P., Reignault, P., Halama, P., 2018. Biocontrol of the wheat pathogen Zymoseptoria tritici using cyclic lipopeptides from Bacillus subtilis. Environ. Sci. Pollut. Res. 25, 29822–29833. https://doi.org/10.1007/s11356-017-9241-9.

Moyne, A.L., Shelby, R., Cleveland, T.E., Tuzun, S., 2001. Bacillomycin D: an iturin with antifungal activity against Aspergillus flavus. J. Appl. Microbiol. 90, 622–629. https://doi.org/10.1046/j.1365-2672.2001.01290.x.

Mu, F., Chen, X., Fu, Z., Wang, X., Guo, J., Zhao, X., Zhang, B., 2023. Genome and transcriptome analysis to elucidate the biocontrol mechanism of Bacillus amyloliquefaciens XJ5 against Alternaria solani. Microorganisms 11, 2055. https://doi.org/10.3390/microorganisms11082055.

Muchembled, J., Deweer, C., Sahmer, K., Halama, P., 2018. Antifungal activity of essential oils on two Venturia inaequalis strains with different sensitivities to tebuconazole. Environ. Sci. Pollut. Res. 25, 29921–29928. https://doi.org/10.1007/s11356-017-0507-z.

Nasir, M.N., Besson, F., 2012. Interactions of the antifungal mycosubtilin with ergosterol-containing interfacial monolayers. Biochim. Biophys. Acta Biomembr. 1818 (5), 1302–1308. https://doi.org/10.1016/j.bbamem.2012.01.020.

Omrane, S., Sghyer, H., Audéon, C., Lanen, C., Duplaix, C., Walker, A.-S., Fillinger, S., 2015. Fungicide efflux and the MgMFS1 transporter contribute to the multidrug resistance phenotype in Zymoseptoria tritici field isolates. Environ. Microbiol. 17, 2805–2823. https://doi.org/10.1111/1462-2920.12781.

Ongena, M., Jacques, P., 2008. Bacillus lipopeptides. versatile Weapons Plant Dis. biocontrol. Trends Microbiol. 16, 115–125. https://doi.org/10.1016/j.tim.2007.12.009.

Ongena, M., Jourdan, E., Adam, A., Paquot, M., Brans, A., Joris, B., Arpigny, J.L., Thonart, P., 2007. Surfactin and fengycin lipopeptides of Bacillus subtilis as elicitors of induced systemic resistance in plants. Environ. Microbiol. 9 (4), 1084–1090. https://doi.org/10.1111/j.1462-2920.2006.01202.x.

Pan, J., Hu, C., Yu, J.-H., 2018. Lipid biosynthesis as an antifungal target. J. Fungi 4, 50. https://doi.org/10.3390/jof4020050.

Price, C.L., Parker, J.E., Warrilow, A.G., Kelly, D.E., Kelly, S.L., 2015. Azole fungicides – understanding resistance mechanisms in agricultural fungal pathogens. Pest. Manag. Sci. 71, 1054–1058. https://doi.org/10.1002/ps.4029.

Rahman, A., Uddin, W., Wenner, N.G., 2015. Induced systemic resistance responses in perennial ryegrass against Magnaporthe oryzae elicited by semi-purified surfactin lipopeptides and live cells of Bacillus amyloliquefaciens. Mol. Plant Pathol. 16, 546–558. https://doi.org/10.1111/mpp.12209.

Richter, M., Rosselló-Móra, R., Oliver Glöckner, F., Peplies, J., 2016. JSpeciesWS: a web server for prokaryotic species circumscription based on pairwise genome comparison. Bioinformatics 32, 929–931. https://doi.org/10.1093/bioinformatics/btv681.

Rocafort, M., Srivastava, V., Bowen, J.K., Díaz-Moreno, S.M., Guo, Y., Bulone, V., Plummer, K.M., Sutherland, P.W., Anderson, M.A., Bradshaw, R.E., Mesarich, C.H., 2023. Cell Wall Carbohydrate Dynamics during the Differentiation of Infection Structures by the Apple Scab Fungus, Venturia inaequalis. Microbiol. Spectr. 11 (3), e0421922 https://doi.org/10.1128/spectrum.04219-22.

Romero, D., de Vicente, A., Rakotoaly, R.H., Dufour, S.E., Veening, J.-W., Arrebola, E., Cazorla, F.M., Kuipers, O.P., Paquot, M., Pérez-García, A., 2007. The Iturin and Fengycin families of lipopeptides are key factors in antagonism of Bacillus subtilis towards Podosphaera fusca. Mol. Plant Microbe Interact. 20, 430–440. https://doi.org/10.1094/MPMI-20-4-0430.

Schmittgen, T.D., Livak, K.J., 2008. Analyzing real-time PCR data by the comparative CT method. Nat. Protoc. 3, 1101–1108. https://doi.org/10.1038/nprot.2008.73.

Schnabel, G., Jones, A.L., 2001. The 14α-Demethylase (CYP51A1) Gene is Overexpressed in Venturia inaequalis Strains Resistant to Myclobutanil. Phytopathology 91, 102-110. https://doi.org/10.1094/PHYTO.2001.91.1.102.

Shirane, N., Takenaka, H., Ueda, K., Hashimoto, Y., Katoh, K., Ishii, H., 1996. Sterol analysis of DMI-resistant and sensitive strains of Venturia inaequalis. Phytochemistry 41, 1301–1308. https://doi.org/10.1016/0031-9422(95)00787-3.

Siah, A., Tisserant, B., El Chartouni, L., Duyme, F., Deweer, C., Roisin-Fichter, C., Sanssené, J., Durand, R., Reignault, P., Halama, P., 2010. Mating type idiomorphs from a French population of the wheat pathogen Mycosphaerella graminicola: widespread equal distribution and low but distinct levels of molecular polymorphism. Fungal Biol. 114, 980–990. https://doi.org/10.1016/j.funbio.2010.09.008.

Stammler, G., Cordero, J., Koch, A., Semar, M., Schlehuber, S., 2009. Role of the Y134F mutation in cyp51 and overexpression of cyp51 in the sensitivity response of Puccinia triticina to epoxiconazole. Crop Prot. 28, 891–897. https://doi.org/10.1016/j.cropro.2009.05.007.

Stephenson, S.L., 2010. The Kingdom fungi: the biology of mushrooms, molds, and lichens. Timber Press, Portland.

Sun, X., Xu, Q., Ruan, R., Zhang, T., Zhu, C., Li, H., 2013. PdMLE1, a specific and active transposon acts as a promoter and confers Penicillium digitatum with DMI resistance. Environ. Microbiol. Rep. 5, 135–142. https://doi.org/10.1111/1758-2229.12012.

Talebi, A., de Laat, V., Spotbeen, X., Dehairs, J., Rambow, F., Rogiers, A., Vanderhoydonc, F., Rizotto, L., Planque, M., Doglioni, G., Motamedi, S., Nittner, D., Roskams, T., Agostinis, P., Bechter, O., Boecxstaens, V., Garmyn, M., O'Farrell, M., Wagman, A., Kemble, G., Leucci, E., Fendt, S.-M., Marine, J.-C., Swinnen, J.V., 2023. Pharmacological induction of membrane lipid polyunsaturation sensitizes melanoma to ROS inducers and overcomes acquired resistance to targeted therapy. J. Exp. Clin. Cancer Res. 42, 92. https://doi.org/10.1186/s13046-023-02664-7.

Tan, S.T., Ramesh, T., Toh, X.R., Nguyen, L.N., 2020. Emerging roles of lysophospholipids in health and disease. Prog. Lipid Res. 80, 101068 https://doi.org/10.1016/j.plipres.2020.101068.

Todd, B.L., Stewart, E.V., Burg, J.S., Hughes, A.L., Espenshade, P.J., 2006. Sterol regulatory element binding protein is a principal regulator of anaerobic gene expression in fission yeast. Mol. Cell Biol. 26, 2817–2831. https://doi.org/10.1128/MCB.26.7.2817-2831.2006.

Van Meer, G., Voelker, D.R., Feigenson, G.W., 2008. Membrane lipids: where they are and how they behave. Nat. Rev. Mol. Cell Biol. 9, 112–124. https://doi.org/10.1038/nrm2330.

Vanittanakom, N., Loeffler, W., Koch, U., Jung, G., 1986. Fengycin-A novel antifungal lipopeptide antibiotic produced by Bacillus subtilis F-29-3. J. Antibiot. 39, 888–901. https://doi.org/10.7164/antibiotics.39.888.

Vassaux, A., Rannou, M., Peers, S., Daboudet, T., Jacques, P., Coutte, F., 2021. Impact of the purification process on the spray-drying performance of three families of lipopeptide biosurfactants produced by Bacillus subtilis. Front. Bioeng. Biotechnol. 9, 815337 https://doi.org/10.3389/fbioe.2021.815337.

Vijaya Palani, P., Lalithakumari, D., 1999. Resistance of Venturia inaequalis to the sterol biosynthesis inhibiting fungicide, penconazole [1-(2-(2,4-dichlorophenyl) pentyl)-1H-1,2,4-triazole. Mycol. Res. 103, 1157–1164. https://doi.org/10.1017/S0953756299008321.

Villani, S.M., Biggs, A.R., Cooley, D.R., Raes, J.J., Cox, K.D., 2015. Prevalence of myclobutanil resistance and difenoconazole insensitivity in populations of Venturia inaequalis. Plant Dis. 99, 1526–1536. https://doi.org/10.1094/PDIS-01-15-0002-RE.

Villani, S.M., Hulvey, J., Hily, J.-M., Cox, K.D., 2016. Overexpression of the CYP51A1 gene and repeated elements are associated with differential sensitivity to DMI fungicides in Venturia inaequalis. Phytopathology 106, 562–571. https://doi.org/10.1094/PHYTO-10-15-0254-R.

Weete, J.D., 2012. Lipid Biochemistry of Fungi and Other Organisms. Springer New York.

Willger, S.D., Puttikamonkul, S., Kim, K.-H., Burritt, J.B., Grahl, N., Metzler, L.J., Barbuch, R., Bard, M., Lawrence, C.B., Jr, R.A.C., 2008. A Sterol-Regulatory Element Binding Protein Is Required for Cell Polarity, Hypoxia Adaptation, Azole Drug Resistance, and Virulence in Aspergillus fumigatus. PLoS Pathog. 4, e1000200 https://doi.org/10.1371/journal.ppat.1000200.

Wise, C., Falardeau, J., Hagberg, I., Avis, T.J., 2014. Cellular Lipid Composition Affects Sensitivity of Plant Pathogens to Fengycin, an Antifungal Compound Produced by Bacillus subtilis Strain CU12. Phytopathology 104, 1036–1041. https://doi.org/10.1094/PHYTO-12-13-0336-R.

Wood, D.E., Salzberg, S.L., 2014. Kraken: ultrafast metagenomic sequence classification using exact alignments. Genome Biol. 15, R46 https://doi.org/10.1186/gb-2014-15-3-r46.

Xu, X.-M., Gao, L.-Q., Yang, J.-R., 2010. Are insensitivities of Venturia inaequalis to myclobutanil and fenbuconazole correlated. Crop Prot. 29, 183–189. https://doi.org/10.1016/j.cropro.2009.07.002.

Xue, J., Sun, L., Xu, H., Gu, Y., Lei, P., 2023. Bacillus atrophaeus NX-12 utilizes exosmotic glycerol from Fusarium oxysporum f. sp. cucumerinum for fengycin production. J. Agric. Food Chem. 71, 10565–10574. https://doi.org/10.1021/acs.jafc.3c01276.

Yaegashi, H., Hirayama, K., Akahira, T., Ito, T., 2020. Point mutation in CYP51A1 of Venturia inaequalis is associated with low sensitivity to sterol demethylation inhibitors. J. Gen. Plant Pathol. 86, 245–249. https://doi.org/10.1007/s10327-020-00924-4.

Yang, X., Zhang, L., Xiang, Y., Du, L., Huang, X., Liu, Y., 2020. Comparative transcriptome analysis of *Sclerotinia* sclerotiorum revealed its response mechanisms to the biological control agent, Bacillus amyloliquefaciens. Sci. Rep. 10, 12576 https://doi.org/10.1038/s41598-020-69434-9.

Zakharova, A.A., Efimova, S.S., Malev, V.V., Ostroumova, O.S., 2019. Fengycin induces ion channels in lipid bilayers mimicking target fungal cell membranes. Sci. Rep. 9, 16034 https://doi.org/10.1038/s41598-019-52551-5.

Zhang, L., Sun, C., 2018. Fengycins, cyclic lipopeptides from marine strains of Bacillus subtilis, kill the plant pathogenic fungus Magnaporthe grisea by inducing reactive oxygen species production and chromatin condensation. Appl. Environ. Microbiol. 84 (18), e00445 https://doi.org/10.1128/AEM.00445-18.